

2010

Anion Accelerated Semicarbazone Formation with Pyruvamide

Susanta Dan

Follow this and additional works at: <https://ir.lib.uwo.ca/digitizedtheses>

Recommended Citation

Dan, Susanta, "Anion Accelerated Semicarbazone Formation with Pyruvamide" (2010). *Digitized Theses*. 3726.

<https://ir.lib.uwo.ca/digitizedtheses/3726>

This Thesis is brought to you for free and open access by the Digitized Special Collections at Scholarship@Western. It has been accepted for inclusion in Digitized Theses by an authorized administrator of Scholarship@Western. For more information, please contact wlsadmin@uwo.ca.

Anion Accelerated Semicarbazone Formation with Pyruvamide

(Spine Title: Anion Accelerated Semicarbazone
Formation with Pyruvamide)

(Thesis format: Monograph)

by

Susanta Dan

Graduate Program in Chemistry

A thesis submitted in partial fulfillment of the
requirements for the degree

Master of Science

The School of Graduate and Postdoctoral Studies
The University of Western Ontario
London, Ontario, Canada.

© Susanta Dan 2010

CERTIFICATE OF EXAMINATION

Supervisor

Examiners

Dr. James A. Wisner

Dr. Michael A. Kerr

Dr. Mark S. Workentin

Dr. Jin Zhang

The thesis by

Susanta Dan

entitled:

**Anion Accelerated Semicarbazone
Formation with Pyruvamide**

is accepted in partial fulfillment of the
requirements for the degree of
Master of Science

Date _____

Chair of the Thesis Examination Board

Abstract and Keywords

Isophthalamide and pyridine dicarboxamide have been a common motif to anion receptor design. Dynamic combinatorial chemistry has been a fast growing field towards the advancement of receptor design through the use of labile bonds. Schiff bases have been employed as the labile bonding unit of recent receptors.

A pyridine dicarboxamide analogue containing a labile bond *via* a semicarbazone unit was synthesized from the condensation between a semicarbazide and a pyruvamide. Two semicarbazone receptors displayed preferential binding of chloride over other common anions tested (Br^- , HSO_4^- , TsO^- , AcO^- , H_2PO_4^-). It was observed that chloride accelerates the formation of the condensed semicarbazone receptor from 4-hexylsemicarbazide and phenylpyruvamide. Modifications to receptor design *via* the removal of a hydrogen bond donor site brought insight to the role that chloride plays in the mechanism of the condensation reaction. Other anions (HSO_4^- , TsO^- , Br^- , I^- , ClO_4^- , PF_6^- , AcO^-) tested displayed acceleration in semicarbazone formation through hydrogen bonding.

Keywords: Anion recognition, semicarbazone acceleration, isophthalamide, pyridine dicarboxamide, hydrogen bonding, dynamic combinatorial chemistry.

Acknowledgments

I would like to thank Dr. Wisner for the opportunity as it was an enlightening experience on how to design, conduct and manage research. Hopefully I have become a better researcher than when I started.

I would thanks the members of the Wisner Laboratory as they made the time interesting to say the least. Thanks to the Hudson Group for always being there to bounce ideas off of and suggesting alternatives. The Chemistry Department: the staff, technicians, fellow grad students and professors.

The support provided by my family and friends throughout this process was invaluable.

Table of Contents

Certificate Of Examination	ii
Abstract and Keywords.....	iii
Acknowledgments	iv
Table of Figures.....	viii
Table of Schemes	xii
List of Tables.....	xiii
List of Abbreviations	xiv
Chapter 1: Introduction.....	1
1.1 Anion recognition.....	1
1.2 Hydrogen bonding receptors employing N-H donors.	2
1.3 Isophthalamide based receptors.	5
1.4 Templatation in synthesis	13
1.5 Dynamic combinatorial chemistry	20
1.6 Schiff base receptors in DCC.....	21
1.7 Hydrazones receptors in DCC.....	22
1.8 Scope of the Thesis.....	26
Chapter 2.....	27
2.1 Introduction.....	27
2.1.1 Schiff Base	27

2.1.2	Anion acceleration of Schiff base formation of pseudopeptidic macrocycles. ...	30
2.1.3	Lewis Acid catalyzed Schiff base exchange in non-aqueous conditions.	31
2.1.4	Hydrazone containing anion receptors.....	32
2.1.5	Semicarbazone containing anion receptors	34
2.2	Results and Discussion	35
2.2.1	Synthesis.....	36
2.2.2	Titrations with semicarbazone receptors.....	39
2.2.3	Anion acceleration of semicarbazone formation.	48
2.2.4	Summary and Conclusions.....	56
2.3	Experimental	57
Chapter 3.....		67
3.1.	Introduction.....	67
3.2.	Results and Discussion	70
3.2.1	Synthesis.....	70
3.2.2	Kinetics – removal of hydrogen bond donors.	75
3.2.3	Kinetics of Schiff base formation in the presence of TBACl.....	81
3.2.4	Kinetics of semicarbazone formation with various anions	87
3.2.5	Summary and Conclusions.....	91
3.3.	Experimental	93
Bibliography.....		100

Curriculum Vitae.....105

Table of Figures

Chapter 1

Figure 1.1 - Amine based receptors: octaazacryptand (left), bis(tren) (middle), and macrobicyclic azaphane (right).....	3
Figure 1.2 - Bisurea receptor of Brooks (left), mono-urea receptor of Amendola (centre) and crown modified receptor (right).....	4
Figure 1.3 - Huang's molecular switch.	5
Figure 1.4 - Isophthalamide unit: <i>syn-syn</i> geometry (left), <i>syn-anti</i> geometry (left-centre) <i>anti-anti</i> geometry (right-centre) and pyridine dicarboxamide (right).....	7
Figure 1.5 - Modified isophthalamide structures: Smith's Lewis acid (left), sulfonamide (centre), and <i>N</i> -ethylhydroxysulfonamide (right).	7
Figure 1.6 - Example of Smith's ditopic receptor (left) and Hamilton's barbiturate receptor where 'Y' is a linker (right).....	9
Figure 1.7 - Isophthalamide macrocycle, two-unit (above) and four-unit (below) binding quinone.....	10
Figure 1.8 - Isophthalamide macrocycle with alkyl linker and internal hydrogen bonding (left) and pre-organized analog (right).	11
Figure 1.9 - Leigh's molecular shuttle.	12
Figure 1.10 - Smith's protected squaraine.....	13
Figure 1.11 - Example of Beer's anion-templated pseudorotaxane (R = hexyl).	14
Figure 1.12 – Example of clipping approach to rotaxane formation.....	15
Figure 1.13 - Ramos's Macrocycle.	16
Figure 1.14 – Hasenknof's circular helicate.	16
Figure 1.15 - Amidinothiourea metallacage with anion X ⁻ in the centre.....	18

Figure 1.16 - Vögtle's trapping method towards a [2]rotaxane.....	19
Figure 1.17 - Stoddart's Dynamic [2]rotaxanes.....	20
Figure 1.18 – Sanders's peptide hydrazide monomer unit.	23
Figure 1.19 - Dynamic Barbiturate Receptor.....	24
Figure 1.20 – Sessler's aldehyde (left) and amine (right) sources for polypyrrolic macrocycles.	25
Figure 1.21 – Pyridine dicarboxamide (left) and dynamic receptor examined in this thesis (right).	26

Chapter 2

Figure 2.1 - General mechanism of imine formation.	27
Figure 2.2 – Proposed intermediates towards carbinolamine formation.	29
Figure 2.3 - Solvent and catalyst assisted proton transfers in carbinolamine formation. ...	30
Figure 2.4 - Pseudopeptidic macrocycle binding terephthalate.	31
Figure 2.5 - Gupta's (left) and Wang's (right) hydrazone receptor.....	33
Figure 2.6 - Chawla's calix with a lower (left) and an upper (right) rim binding site.	34
Figure 2.7 - Retrosynthesis of a semicarbazone.....	35
Figure 2.8 - Structure of semicarbazide 8b.....	37
Figure 2.9 - Semicarbazone receptor with desired binding conformation (left), alternate binding conformation (middle) and pyridine dicarboxamide analogue (right).....	40
Figure 2.10 - ROESY ¹ H NMR of Phenylamido-hexylsemicarboxide 10-ba.....	41
Figure 2.11 – Example of the change in chemical shift upon host-guest (10-ba TBACl) binding.	43

Figure 2.12 – Two possible conformations of semicarbazone receptors 10 with anions – Isophthalamide-like (left) and Urea-like (right) conformations.....	46
Figure 2.13 - ¹ H NMR spectra in CDCl ₃ of pure pyruvamide and condensed semicarbazone (10-ba).....	49
Figure 2.14 - Spectra of condensation between phenylpyruvamide (9b) and 4-hexylsemicarbazide (8a) in the presence of 1 equivalent of TBACl at various time intervals.....	50
Figure 2.15 - Concentration of product from condensation reaction between phenylpyruvamide (20 mM) and 4-hexylsemicarbazide (20 mM) with 1 equivalent of TBACl over time with a line representing the best fit for the first eight points.	52
Figure 2.16 - Percent of receptor 10-ba formation over initial 140 minutes with 0 – 4 equivalents of TBACl added.....	53
Figure 2.17 - Percent formation of receptor 10-ba over time with 0 – 4 equivalents of TBACl added.	53
Figure 2.18 - Plot of natural logs of initial rates versus concentrations of TBACl.....	55

Chapter 3

Figure 3.1 - Soluble condensed semicarbazone receptors.....	67
Figure 3.2 - Structure of modified semicarbazone receptors (periphery) and original receptor (centre).	68
Figure 3.3 - Modified reactants for condensation reaction.	69
Figure 3.4 - Pyridine dicarboxamide (left) and Schiff base receptor 17 (right).....	70
Figure 3.5 - Methylated and unmethylated components towards semicarbazone formation.....	76

Figure 3.6 - ¹ H Spectra of phenylpyruvamide, 9b and 4,4-butylmethylsemicarbazide, 14 in CDCl ₃ at 298K.....	78
Figure 3.7 - Acceleration of semicarbazone condensation (9b + 14) in the presence of TBACl.....	79
Figure 3.8 - Intermediates of dehydration process: 5-membered ring (left) and pseudo-6-membered ring (right).....	80
Figure 3.9 - Percent conversion from phenylpyruvamide to condensed receptor 17.....	82
Figure 3.10 - Plot of natural logs of initial rates versus concentration of TBACl for Schiff base receptor 17.....	83
Figure 3.11 – Initial percent semicarbazone conversion from phenylpyruvamide in the presence of 1 eq. of TBAX.	89
Figure 3.12 - Overall percent conversion of semicarbazone from phenylpyruvamide in the presence of 1 eq. of TBAX.	90

Table of Schemes

Chapter 2

Scheme 2.1 – Synthesis of semicarbazide 8a.....	36
Scheme 2.2 – Synthesis of pyruvamides 9a,b.....	37
Scheme 2.3 - Synthesis of condensed semicarbazone receptors.....	38
Scheme 2.4 - Semicarbazone (10-ba) formation in the presence of chloride	48

Chapter 3

Scheme 3.1 - Synthetic route of <i>N</i> -Methylphenyl pyruvamide.....	71
Scheme 3.2 - Synthetic route of 4,4-Butylmethylsemicarbazide.....	72
Scheme 3.3 - Synthetic route to 2-amino- <i>N</i> -hexylacetamide.....	73
Scheme 3.4 - Route to Schiff base receptor.....	74
Scheme 3.5 - Possible condensation mechanism of semicarbazone formation.....	75
Scheme 3.6 – Equilibrium between 5-membered ring (top left) and pseudo-6-membered (bottom right) internal hydrogen bonding rings.....	86
Scheme 3.7 - Dehydration steps of phenylpyruvamide and hexylamine (R = Hexyl).....	87

List of Tables

Table 1 - Association constants K_a (M^{-1}) in CD_2Cl_2 of selected isophthalamide and pyridine dicarboxamide.	6
Table 2 - Association constants of 10-ba with various TBA salts in $CDCl_3$ at 298K.....	45
Table 3 - Association constants determined for 10-aa with various TBA salts in $CDCl_3$ at 298K.	47
Table 4 – Increase in initial rates of formation of 10-ba in the presence of different amounts of TBACl.	54
Table 5 - Increase in initial rates of formation for receptor 17 in the presence of various TBACl equivalents.	81
Table 6 – Summary of initial rates of reaction.....	84
Table 7 - Rate of semicarbazone (10-ba) formation with various TBA salts.	88

List of Abbreviations

Abbreviation

Defenition

10-CSA	10-camphorsulfonic acid
CDCl_3	Deuterated chloroform
d	doublet
DCC	<i>N,N</i> -Dicyclocarbodiimide
DCC	Dynamic combinatorial chemistry
DCM	Dichloromethane
DMSO	Dimethylsulfoxide
eq	Equivalent
ESI LRMS	electrospray ionization low resolution mass spectrometry
EtOH	Ethanol
FCC	flash column chromatography
ΔG	change in Gibbs free energy
h	hours
<i>H</i> -bonding	hydrogen bonding
HCl	Hydrochloric acid
HRMS	High resolution mass spectrometry

Hz	Hertz
δ	chemical shift in parts per million
K	Kelvin
kJ	Kilojoules
M	Molar, moles per litre
m	multiplet
MeOH	Methanol
MHz	Megahertz
min	minutes
mL	milliliter
mmol	millimole
mol	mole
ppm	parts per million
POCl_3	Phosphorous oxychloride
q	quartet
quant	Quantitative
RBF	Round-bottomed flask

ROESY	Rotational Frame Nuclear Overhauser Effect Spectroscopy
s	singlet
t	triplet
TBACl	Tetrabutylammonium chloride
TFA	Trifluoroacetic acid
TsO ⁻	<i>p</i> -Toluensulfonate
μL	microlitre

Chapter 1: Introduction

1.1 Anion recognition

The interest in and development of receptors for anions and anionic species has gained momentum over the past 20 years. Anions are an essential part of biological systems and also have an impact upon the environment. Chloride channels, for example, are used to maintain electrochemical gradients across membranes and genetic defects to these channels can result in various diseases such as Bartter's syndrome, Dent's disease¹ and cystic fibrosis.² In the environment, phosphate and nitrate can lead to eutrophication of inland waterways and lakes as a result from the overuse of fertilizers.³ The importance in the detection and identification of anions has led to the development of synthetic anion receptors. These receptors could reveal the presence of anions through electrochemical,⁴ photoinduced,⁵ or optical^{6,7} means. The first encapsulation of a halide anion was reported by Park and Simmons in 1968.⁸ In this case, a halide anion was encapsulated by a diprotonated bicyclic katapinand through hydrogen bonding.

Hydrogen bonds are one example of the non-covalent interactions that are employed in the binding between a guest species and its host receptor. Dipole-dipole, cation- π interactions, and π - π stacking are some of the other forces utilized in host-guest association, though hydrogen bonding is directional and one of the strongest;⁹ hence it is common in receptor design.

The binding of an anion by a receptor can vary based upon the number of hydrogen bond donors (amine or amide), presence of formal charge, dimensionality

(monocycle or bicycle) of the receptor, and the topology of the anion. Anions can come in various shapes and sizes, so receptors are designed to match these variances wherever possible.¹⁰ Similar to transition metals, anions can adopt different geometries for coordination that arise from the number of hydrogen bond interactions (two to nine) observed with its receptor.¹¹ Anions can be classified by their shape: spherical, linear, V-shaped, trigonal-planar, and tetrahedral to name a few. Halides, spherical anions, can accept two to nine coordinating hydrogen bonds. There are few examples of linear anion reception observed, one exception being the encapsulation of an azide by an octaazacryptand. Nitrite and acetate are V-shaped and generally accept two to five coordinating hydrogen bonds with a maximum of eight. Nitrate on the other hand, a trigonal-planar anion, has only been seen to accept two or three hydrogen bonds. Lastly, tetrahedral anions like sulfate or phosphate accept between six and eight hydrogen bonds.

1.2 Hydrogen bonding receptors employing N-H donors.

Common functional groups chosen as hydrogen bond donors in receptors are amines, ureas, amides and sulfonamides. Amine/ammonium-based macrobicycles such as octaazacryptand and bis(tren), have been shown to have high binding constants for fluoride and chloride. As a result, Ilioudis *et al* sought to incorporate this design towards a new macrobicyclic azaphane receptor¹² (Figure 1.1).

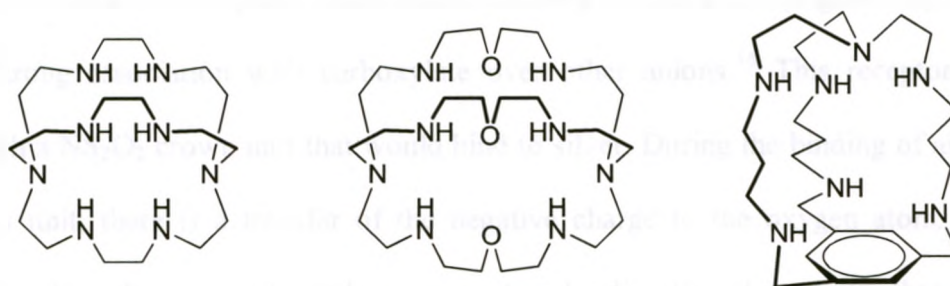


Figure 1.1 - Amine based receptors: octaazacryptand (left), bis(tren) (middle), and macrobicyclic azaphane (right).

It is generally observed that the amines provide better binding when protonated as observed with the binding of azaphane with four anions (F^- , Cl^- , Br^- , NO_3^-) as sodium salts at different states of protonation. In all states, the binding of fluoride was higher than chloride. However, there were no observable changes in the presence of bromide or nitrate.

Urea, another hydrogen bond donor unit, was first described in the binding of anions by Smith and co-workers in 1992.¹³ Here the strongest association in chloroform was observed with acetate anions followed by phosphorous oxyanions and sulfur oxyanions. In 1993, Fan *et al.* continued to show the binding of carboxylate anions by the urea motif.¹⁴ This would be the start of further use of ureas in receptor design.

Strong binding of carboxylates by urea complexes has been observed with receptors designed recently. Brooks *et al* have shown strong preference for carboxylates over chloride, bromide, hydrogensulfate and dihydrogenphosphate.¹⁵ Their receptor

contained two urea units (Figure 1.2) that still formed 1:1 complexes with carboxylate anions. Amendola and colleagues showed that with only one urea unit (Figure 1.2), there is still a strong association with carboxylate over other anions.¹⁶ This receptor was coupled with a NS₂O₂ crown unit that would bind to silver. During the binding of anions by the urea unit, there is a transfer of the negative charge to the oxygen atom. This increased negative charge results in the oxygen atom binding the silver centre through a conformational change in the receptor. The receptor binds anions more strongly in the presence of silver. Not only does the binding of anions by urea create this silver-oxygen bond, but the bonding between the silver and oxygen also increases the polarization of the N-H of the urea unit. The increase in polarization results in increased hydrogen bonding interactions.

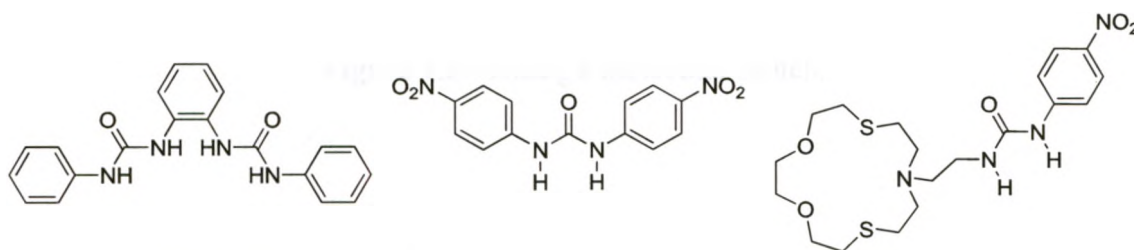


Figure 1.2 - Bisurea receptor of Brooks (left), mono-urea receptor of Amendola (centre) and crown modified receptor (right).

As a result of strong associations with anions, the urea motif has been included with ferrocene to allow electrochemical detection of anions.¹⁷ Detection and association values were higher when two urea units were included in the receptor design, compared

to one. Huang *et al* also developed a molecular switch (Figure 1.3) consisting of a macrocycle interpenetrated with an axle containing two binding sites (composed of a urea and a carbamate).¹⁸ In the presence of acetate, the urea unit would preferentially bind the carboxylate anion while the macrocycle centred itself on the carbamate. When the acetate was not present, the macrocycle would switch to binding the urea unit.

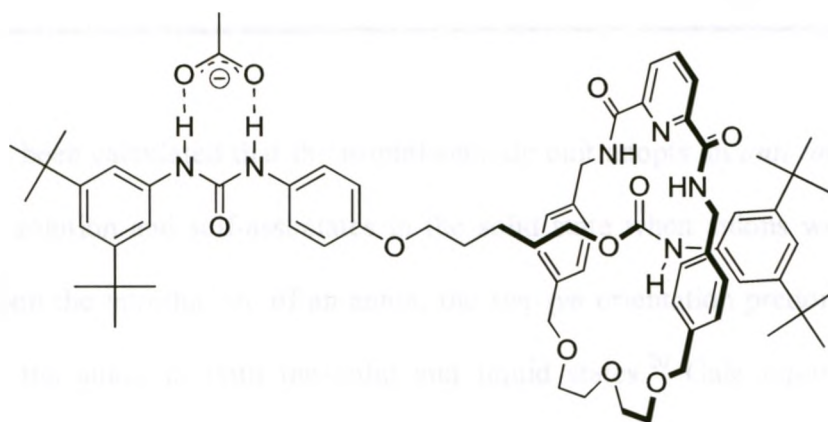


Figure 1.3 - Huang's molecular switch.

1.3 Isophthalamide based receptors.

Amides have been shown to be efficient on their own in the binding of anions. One classic and much studied model of this is the isophthalamide motif. Crabtree and co-workers reported the first use of this structural design for the binding of halides. The binding association values were determined with various anions (F^- , Cl^- , Br^- , I^- , AcO^-), chloride giving the highest value (Table 1).¹⁹

Table 1 - Association constants K_a (M^{-1}) in CD_2Cl_2 of selected isophthalamide and pyridine dicarboxamide.

Anion	Isophthalamide: R, R' = <i>p</i> -(<i>n</i> -Bu) C_6H_4	Diphenylpyridine dicarboxamide
F ⁻	30,000	24,000
Cl ⁻	61,000	1,500
Br ⁻	7,100	57
I ⁻	460	<20
AcO ⁻	19,800	525

It has been calculated that the isophthalamide unit adopts an *anti-anti* or *syn-anti* geometry in solution and self-associates in the solid state when anions were excluded. However, upon the introduction of an anion, the *syn-syn* orientation predominates while coordinating the anion in both the solid and liquid states.²⁰ Gale reported a helical structure forming from the binding of two isophthalamide units and two fluoride ions.²¹ The pyridinedicarboxamide version (Figure 1.4) would overcome problems of self-association as the nitrogen of the pyridine ring would hydrogen bond with both amides bringing about a stabilized *syn-syn* conformation.¹⁹ Eventhough the binding cavity is pre-organized to the desired conformation, the binding of anions was decreased compared to the original isophthalamide unit. This is due to the lone pair electrons on the nitrogen of the pyridine ring repelling larger anions while the smallest, fluoride, was still capable of associating with the receptor.

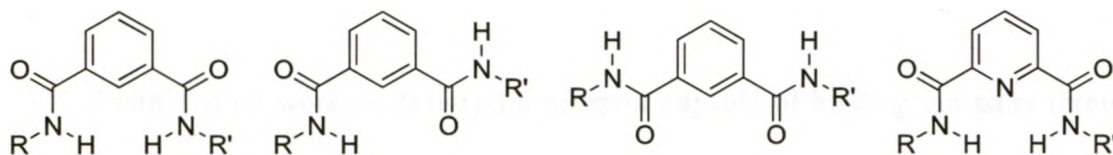


Figure 1.4 - Isophthalamide unit: *syn-syn* geometry (left), *syn-anti* geometry (left-centre) *anti-anti* geometry (right-centre) and pyridine dicarboxamide (right).

Smith and co-workers have also designed a receptor with the isophthalamide motif that was pre-organized in the *syn-syn* orientation. This motif was achieved by the addition of an internal Lewis acid (Figure 1.5) that coordinated with the amide oxygen, which resulted in an increase in association with acetate.²² Other modifications (Figure 1.5) include the use of a sulfonamide¹⁹ and *N*-ethylhydroxysulfonamide²³ where slight increases in binding towards larger anions are observed compared to diphenylisophthalamide. The isophthalamide motif has not only been employed to bind solely anions, but with the incorporation of other key structures has been observed to bind ion pairs and barbiturates, among other guests.

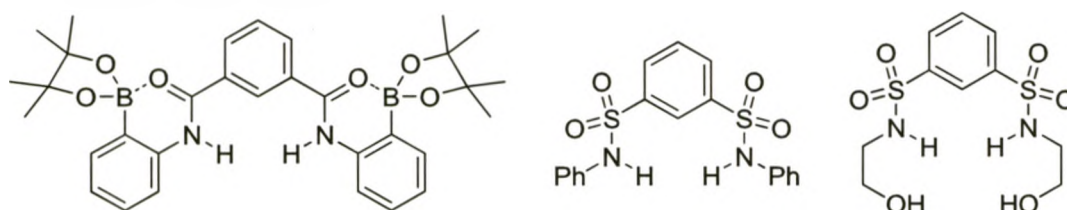


Figure 1.5 - Modified isophthalamide structures: Smith's Lewis acid (left), sulfonamide (centre), and *N*-ethylhydroxysulfonamide (right).

Smith and co-workers designed a receptor capable of binding ion pairs through the use of an isophthalamide and crown ether motif binding anionic and cationic species respectively²⁴ (Figure 1.6). They were able to show the extraction of alkali metal halide salts from an aqueous solution into chloroform. Sodium chloride/bromide and potassium chloride/bromide were extracted as a contact pair within the receptor, while lithium chloride/bromide was extracted with an intervening water molecule between the two ions.²⁵ Binding of alkylammonium salts ($\text{Bu}_4\text{N}^+\text{Cl}^-$, $n\text{-PrNH}_3^+\text{Cl}^-$, $i\text{-PrNH}_3^+\text{Cl}^-$, $\text{Et}_2\text{NH}_2^+\text{Cl}^-$) with this same ditopic receptor showed that smaller ammonium ions resulted in significantly higher binding.²⁶ This is a result of the smaller ions being able to penetrate further into the receptor cavity.

The binding of barbiturates displays the possibility of binding structures other than halide salts. Barbiturates are commonly used as sedatives and anticonvulsants. Hamilton and co-workers employed the isophthalamide motif with the addition of 2,6-diaminopyridine as the amine source for amide formation.²⁷ This added feature increases the number of hydrogen bonding sites available (Figure 1.6). The 5,5-positions of barbiturates are generally substituted and most of the binding interactions occur through the two imide N-Hs and the three carbonyl oxygens.

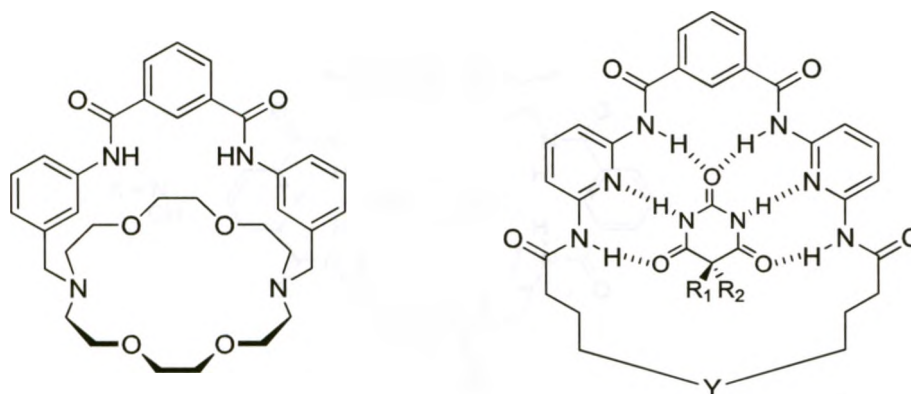


Figure 1.6 - Example of Smith's ditopic receptor (left) and Hamilton's barbiturate receptor where 'Y' is a linker (right).

The binding of other molecules with the isophthalamide motif allows for a vast array of elaborate supramolecular structures that can be designed. An example of this is a macrocyclic structure synthesized by Hunter and co-workers that contains two isophthalamide units (Figure 1.7).²⁸ In their study, the macrocycle was able to encapsulate and bind one quinone molecule. Modifications were made to the macrocycle whereby pyridine was incorporated.

Again as similarly seen by Crabtree with anions, there was slightly reduced binding observed with the pyridine analog. However, Hunter *et al.* also synthesized a four-unit macrocycle whereby two isophthalamide units and two pyridine analogs were incorporated (Figure 1.7). In this structure, binding was observed with the pyridine version containing a pre-organized binding site.

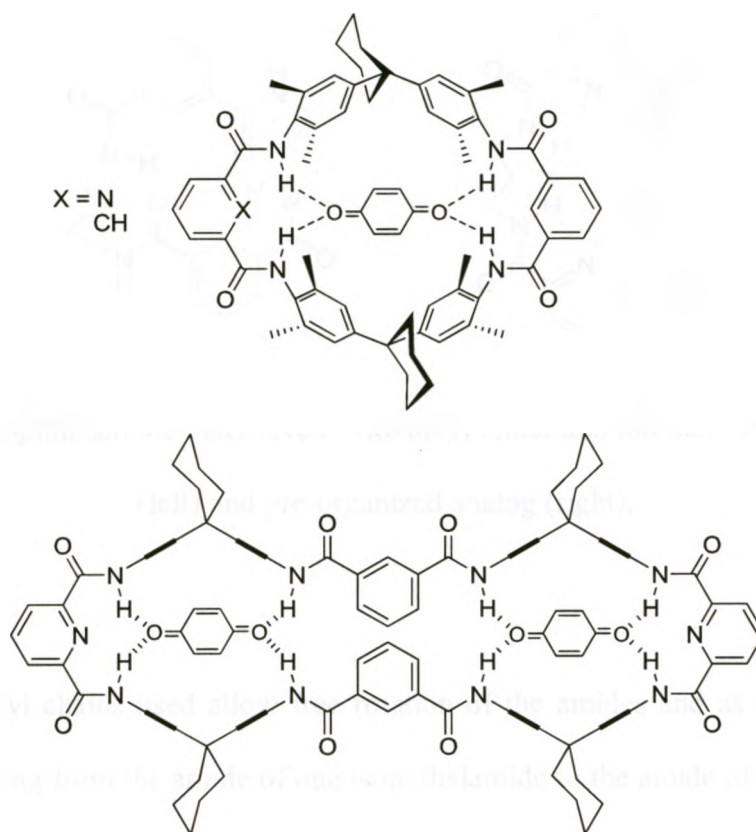


Figure 1.7 - Isophthalamide macrocycle, two-unit (above) and four-unit (below) binding quinone.

The pyridine based binding site pre-arranges the amides into a *syn-syn* conformation for a preferred coordination pocket compared to the anti-anti configuration of the isophthalamide units. Chmielewski *et al* have similarly observed the importance of the pre-organized amide conformations. Two isophthalamide units are connected by various sized alkyl linkers (ethyl to pentyl).²⁹

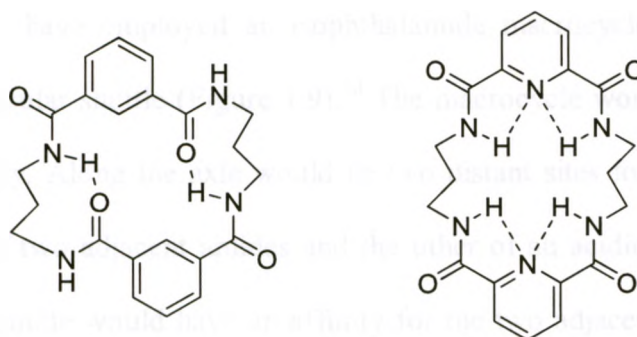


Figure 1.8 - Isophthalamide macrocycle with alkyl linker and internal hydrogen bonding (left) and pre-organized analog (right).

The alkyl chains used allow free rotation of the amides and as a result internal hydrogen bonding from the amide of one isophthalamide to the amide of the other would occur (Figure 1.8). The pyridine unit helps avoid the internal hydrogen bonding between amides. Though the hydrogen bonding between the pyridine and the amides reduces the binding for anions,¹⁹ Chmielewski and co-workers found stronger binding by the pyridine based macrocycle than the original isophthalamide.²⁹

Leigh *et al.* have employed an isophthalamide macrocycle in the design and synthesis of a molecular shuttle (Figure 1.9).³⁰ The macrocycle would allow for an axle penetrating its cavity. Along the axle would be two distant sites for hydrogen bonding; one that consists of two adjacent amides and the other of an acidic phenol. As already seen, the isophthalamide would have an affinity for the two adjacent amides. However, upon addition of base, deprotonation of the phenol yields a negatively charged oxygen available for hydrogen bonding resulting in shuttling of the macrocycle to the new position.

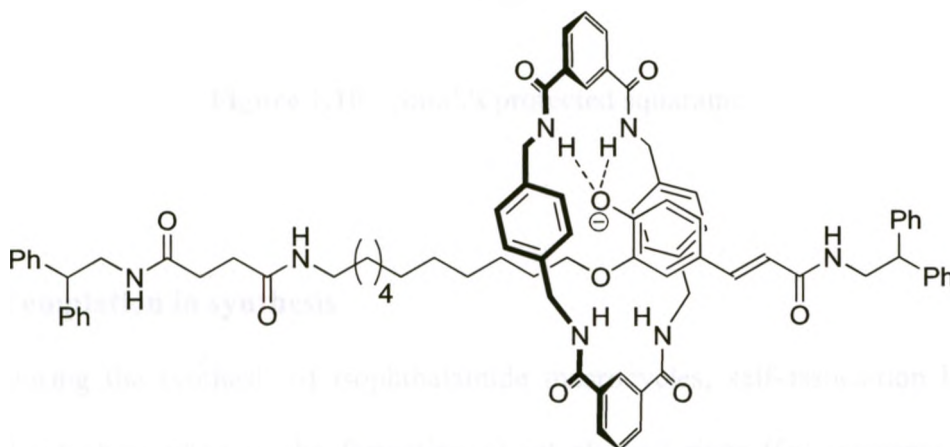


Figure 1.9 - Leigh's molecular shuttle.

A pyridine dicarboxamide macrocycle was used by Smith and co-workers to allow protection of a squaraine based dendrimer dye (Figure 1.10).³¹ The squaraine was protected from chemical attack due to the steric shielding of the large macrocycle. Even

though the dye was encapsulated, it maintained its photophysical properties of high molar absorptivity, narrow absorption/emission, and high fluorescence quantum yield.

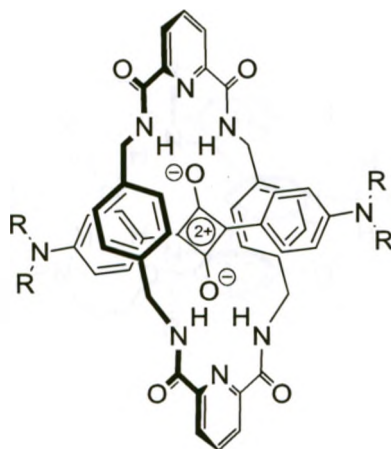


Figure 1.10 - Smith's protected squaraine.

1.4 Templatation in synthesis

During the synthesis of isophthalamide macrocycles, self-association has been observed which resulted in the formation of interlocked rings ($[n]$ -catenanes).³² This aspect of self-association has been used as a template method for the formation of $[2]$ -catenanes.³³ Two isophthalamide units hydrogen bond to each other before ring closing metathesis of the two free alkene termini on each unit with Grubbs's catalyst. Interestingly if the N-H of the isophthalamide units were acylated, then single individual macrocycles were observed.

The strong association of isophthalamide with anions and itself *via* intermolecular interactions have made this motif a versatile unit in the design and synthesis of

supramolecular structures. Beer and co-workers have synthesized various pseudorotaxanes,³⁴ rotaxanes,³⁵ and catenanes³⁶ through anion templation. One example of a pseudorotaxane involved a pyridinium dicarboxamide axle interpenetrating a polyether hydroquinone functionalized isophthalamide macrocycle (Figure 1.11).

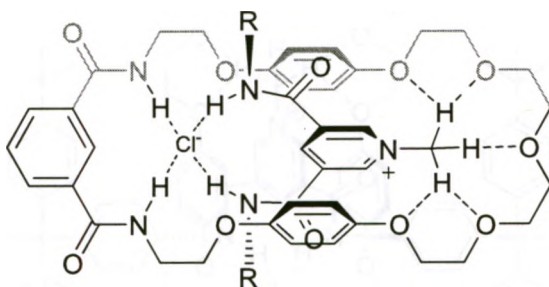


Figure 1.11 - Example of Beer's anion-templated pseudorotaxane (R = hexyl).

There are four hydrogen bonds formed with the chloride, two from the amides of each respective subunit. The π - π stacking between the pyridinium ring and the hydroquinone rings in addition to C-H association with the polyether of the macrocycle, is an additional interaction that helps to stabilize the assembly. Increasing the size of the anions (Br^- , I^- , PF_6^-) results in reduced values of association. The same key structures of the pseudorotaxanes seen in Figure 1.11 were employed in the design of additional rotaxanes and catenanes. In the formation of the rotaxanes, a clipping approach was employed (Figure 1.12). Here, the axle possesses large terminal units that would sterically block the macrocycle from sliding "off" upon rotaxane formation. When a clipping approach is used towards the synthesis of a rotaxane, a strong mode of association between the two components is essential. In this case, a chloride template

provided the desired interactions. In the presence of a non-coordinative anion, such as hexafluorophosphate, there was no evidence of rotaxane formation.

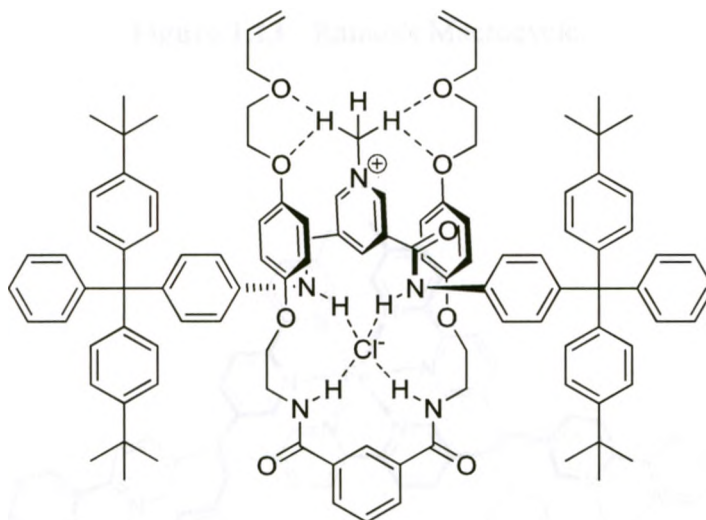


Figure 1.12 – Example of clipping approach to rotaxane formation.

Chloride has also been shown to increase the rate of formation of macrocycles. Ramos and co-workers employed TBACl in accelerating ring closure to the formation of a macrocycle (Figure 1.13)³⁷. The reaction would display first-order rate constants and the reaction rate would be accelerated up to ten times that of un-catalyzed conditions.

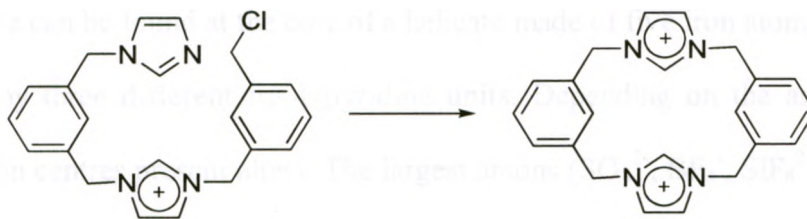


Figure 1.13 - Ramos's Macrocycle.

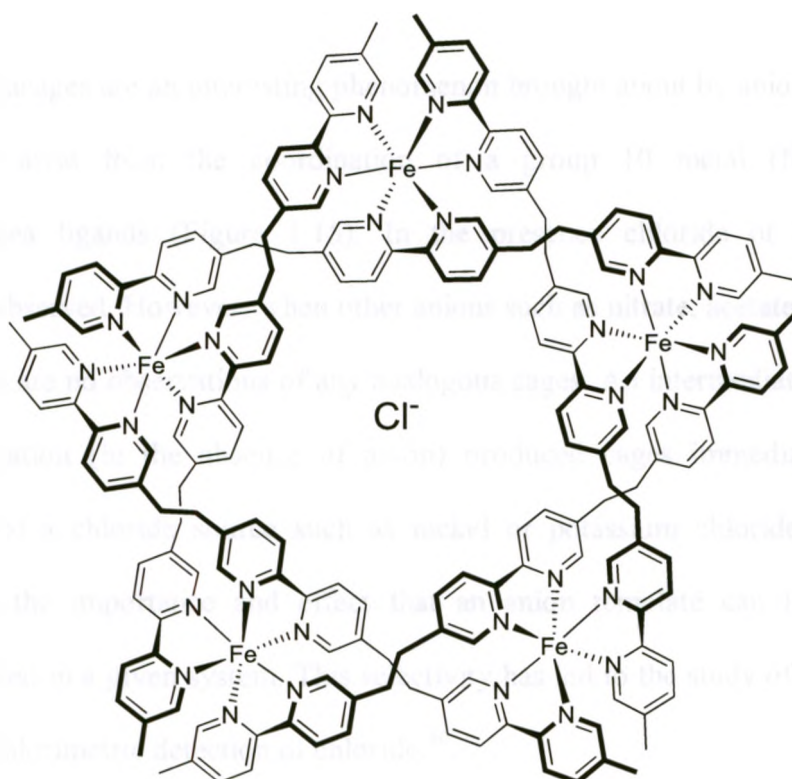


Figure 1.14 – Hasenknopf's circular helicate.

In the formation of circular helicates (Figure 1.14), Hasenknopf and co-workers demonstrated the effects of the choice of template upon formation of a desired product.³⁸ Helicates were synthesised from tris-bipyridine and ferrous chloride with heating. A

single chloride can be found at the core of a helicate made of five iron atoms that are each coordinated by three different tris-bipyridine units. Depending on the anion used, the number of iron centres present alters. The largest anions (SO_4^{2-} , BF_4^- , SiF_6^{2-}) resulted in a six-centred helicate, while an intermediately sized anion (Br^-) yielded a mixture of both the five- and six-centred helicates. When the anion used to form the six-centred structure is removed and replaced with chloride, a change occurs producing the five-centered helicate.

Metallacages are an interesting phenomenon brought about by anion templation.³⁹ These cages arise from the coordination of a group 10 metal (Ni or Pd) by amidinothiourea ligands (Figure 1.15). In the presence chloride or bromide cage formation is observed. However, when other anions such as nitrate, acetate or perchlorate are used there are no observations of any analogous cages. An intermediate present prior to cage formation (in the absence of anion) produced cages immediately after the introduction of a chloride source such as nickel or potassium chloride. This clearly demonstrates the importance and effect that an anion template can have upon the products formed in a given system. This selectivity has led to the study of these cages as a method of colorimetric detection of chloride.⁴⁰

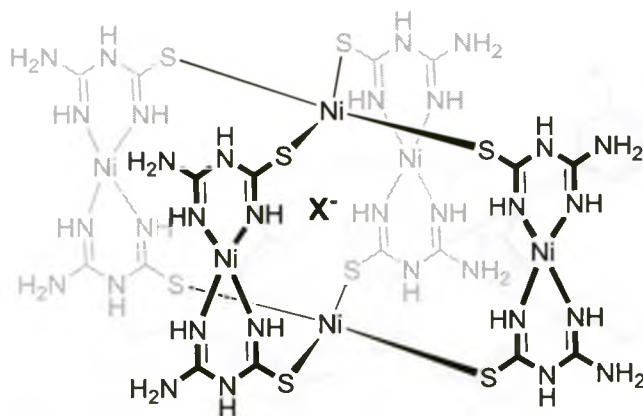


Figure 1.15 - Amidinothiourea metallacage with anion X⁻ in the centre.

The detection of chloride *via* luminescence has been reported by Curiel *et al* through the formation of rhenium(I) containing pseudorotaxanes and rotaxanes.⁴¹ Due to strong affinity of select anions, an analogue of the isophthalamide motif was employed. This strong association of isophthalamide to anionic species is also exemplified in Vögtle's trapping method for [2]rotaxane synthesis (Figure 1.16).⁴² The oxyanion is bound by the macrocycle through hydrogen bonds before attacking the other portion of the axle.

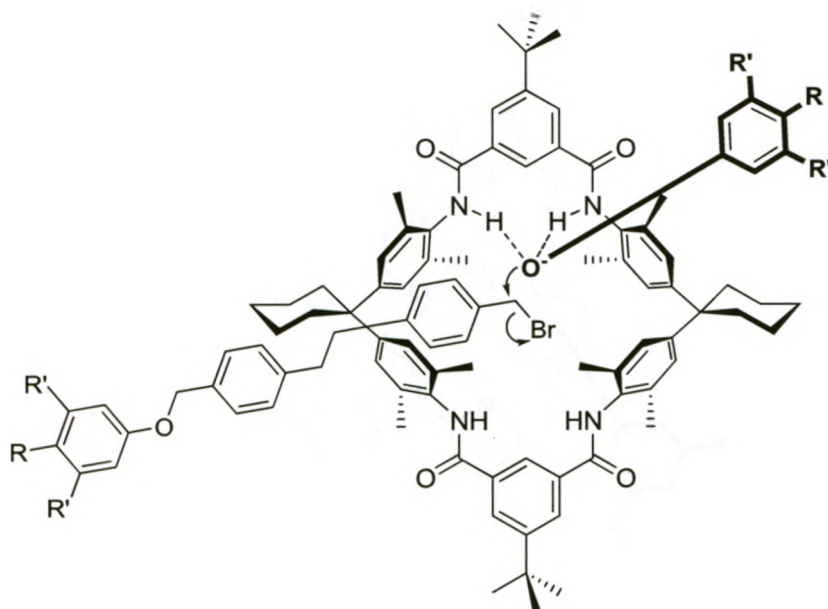


Figure 1.16 - Vögtle's trapping method towards a [2]rotaxane.

Stoddart and co-workers have recently shown another method for the development of a [2]rotaxane that forms reversibly.⁴³ The reversibility can be attributed to the inclusion of dynamic imine bonds in the underlying structure (Figure 1.17) that have previously been used in a “clipping” methodology towards [2]rotaxanes.⁴⁴ In this new approach, varying sizes of the macrocycle: [2 + 2], [3 + 3], [4 + 4] were observed during the condensation of 2,2'-oxybis(ethylamine) with 2,6-diformylpyridine. Only in the presence of the axle template was the [2 + 2] macrocycle observed as the dominant form. Further evidence of the dynamic nature of this structure was found by the introduction of another aldehyde source (4-chloro-2,6-diformylpyridine). After the introduction of this second species, three distinct rotaxanes were observed representing the [2]rotaxanes with zero, one or two chlorides.

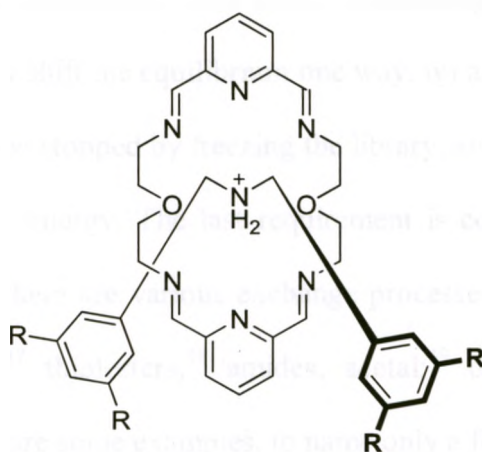


Figure 1.17 - Stoddart's Dynamic [2]rotaxanes.

1.5 Dynamic combinatorial chemistry

The dynamic attribute described in the previous section is integral to a growing field of chemistry known as Dynamic Combinatorial Chemistry (DCC). In brief, the central idea of DCC is that an array of starting materials can reversibly form a variety of products. The dynamic or reversible aspect is due to labile bonds being formed in the products. There are a variety of selection pressures that may be applied during synthesis, such as pH, temperature and templation. This type of thermodynamic selective control has been around since Emil Fischer's studies on carbohydrates and Werner's studies of coordination complexes.⁴⁵ When a template is used, this allows the most suitable receptor to be formed for the substrate in question. DCC allows the possibility of screening through of a multitude of receptors in one step. However, there are a few requirements of

the components (library) used: i) the time of reversibility must be practical, ii) the selection factors and reaction conditions must allow reversibility iii) the conditions must be subtle as not to drastically shift the equilibrium one way, iv) all components need to be soluble, v) the reaction can be stopped by freezing the library, and vi) the members of the library should be of similar energy. The last requirement is commonly avoided in the synthesis of macrocycles. There are various exchange processes employed in DCC,⁴⁵⁻⁴⁶ acyl-based such as esters,⁴⁷ thioesters,⁴⁸ amides; acetal;⁴⁹ disulfide;⁵⁰ Schiff bases, oximines,⁵¹ and hydrazones are some examples, to name only a few.

1.6 Schiff base receptors in DCC

The uses of imines in dynamic combinatorial chemistry were first explored by Huc and Lehn.⁵² A selection of aldehydes and amines were condensed and reduced in the absence and presence of a substrate – carbonic anhydrase II (CA). A variety of products were observed without CA being present. However when the same reaction occurred in the presence of substrate, a change in the distribution of the products was seen.

Schiff bases have also been used in the synthesis of elegant supramolecular structures. Stoddart and co-workers applied this dynamic bond to form stoppers in the synthesis of a [2]rotaxane.⁵³ In the synthesis of another [2]rotaxane Klivansky *et al.* employed π - π stacking interactions between the axle and 1,3,5-benzenetri-aldehyde prior to clipping *via* Schiff base formation.⁵⁴ Imines have been employed in larger structures as seen in the synthesis of hemicarcerands by Stoddart⁵⁵ and Cram.⁵⁶ In the formation of supramolecular structures, Schiff bases have found use in the binding of cationic species.

Jurczak and co-workers created a library based on the condensation of a furan-derived dialdehyde and an aliphatic diaminoether.⁵⁷ Products of the following combinations [1 + 1], [2 + 2], and [3 + 3] were observed, however upon addition of a sodium ion distribution favoured the [1 + 1] species. Addition of 15-crown-5 known to strongly bind sodium swayed the population of the different species back to the original values. Schiff bases have otherwise been commonly observed in the binding of metals.⁵⁸ Coordination with metals have also allowed and helped in the isolation of Schiff bases. In dynamic combinatorial chemistry two other approaches towards the freezing or isolation of products have been employed: reduction to the amine, or trapping *via* Ugi reactions.⁵⁹ In the latter approach, Wessjohann and co-workers had already generated a library of Schiff base products biased towards binding Mg^{2+} or Ba^{2+} prior to ‘freezing’ with an isocyanide and carboxylic acid.

1.7 Hydrazones receptors in DCC

Schiff bases are known to have low stability in neutral or basic aqueous conditions.⁵¹ Oximes and hydrazones are stabilized versions of Schiff bases that do not require reduction or trapping which results in structural changes in receptor products.⁴⁶ Hydrazone exchange is acid catalyzed and, as such, can be switched “off” by the addition of base. A peptide-based hydrazone has received much study by Sanders and co-workers since their first report in 1999.⁶⁰ The underlying structure of these units is a protected aldehyde and a hydrazide on an amino acid core⁶¹ (Figure 1.18). Upon deprotection of the dimethylacetal with trifluoroacetic acid, condensation to the hydrazone occurred, resulting in various sized macrocycles from dimers and trimers, up to hendecamers. The

library was screened for binding to various cationic species and it was observed that in the presence of sodium and especially lithium the population of the trimer significantly increased.

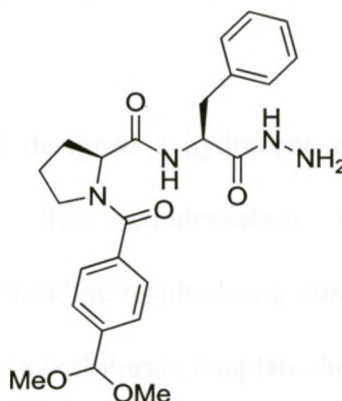


Figure 1.18 – Sanders's peptide hydrazide monomer unit.

In another approach, modifications to the original monomer unit were explored: *meta*-protected aldehyde and a cyclohexyl side chain as compared to the original *para* and phenyl.⁶² Similarly, the introduction of sodium or lithium led to an increase in trimer formation. However, in the *meta*- case, the dimer was predominant in the absence of template and further amplified upon addition of sodium or lithium.

The response and binding towards lithium and sodium led to further studies with ammonium cations.⁶³ The *meta*-acetal was the unit of choice leading to the dimerized species being the major product in the absence of a template. Acetylcholine and *N*-methyl quinuclidinium yielded the highest selectivity and binding with the trimer species. The

formation of a [2]catenane was also observed in the presence of acetylcholine during the condensation of the para-substituted protected peptide.⁶⁴ Self-templating catenanes have also recently been reported.⁶⁵ In place of a peptide core, a steroid *N*-acyl hydrazone has also been studied.⁶⁶ The distribution between dimer and trimer species is dependent on the initial concentration of the monomer. Higher concentrations of monomer led to higher ratios of trimer product.

Lehn and co-workers have designed a hydrazone receptor capable of binding barbiturates (Figure 1.19).⁶⁷ The condensation between 5,5-dimethyl-1,3-cyclohexanedione and 2-hydrazinopyridine resulted in a mixture of various dihydrazone isomers (*Z/Z*, *E/E*, *E/Z*). The use of a barbiturate template during the equilibrium process created a distinct bias with the *Z/Z* isomer being the sole species present.

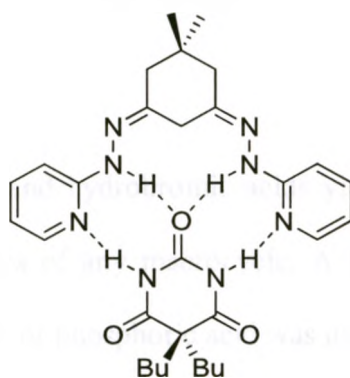


Figure 1.19 - Dynamic Barbiturate Receptor.

There have been very few examples of receptors containing a Schiff base moiety that are capable in binding anionic species. Sessler and co-workers present a polypyrrole

macrocycle capable of binding various anions.⁶⁸ A diformylbipyrrole was condensed with a diamine under acidic conditions (Figure 1.20). The size of the macrocyclic product varied upon the choice of acid, more specifically the resulting conjugate base that was available.

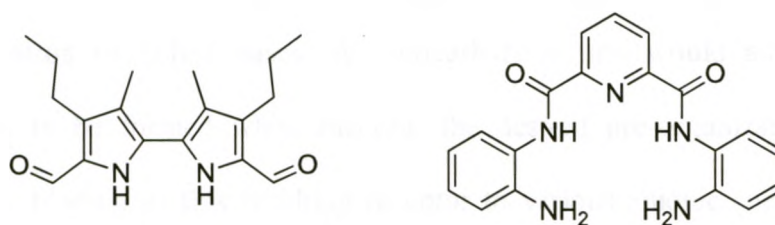


Figure 1.20 – Sessler's aldehyde (left) and amine (right) sources for polypyrrolic macrocycles.

The use of hydrochloric and hydrobromic acids yielded oligomers as the major product and very small quantities of any macrocycle. A [2 + 2] macrocycle appeared when either acetic, trifluoroacetic or phosphoric acid was used with additional by-product oligomers. As with the use of haloacid, nitric acid produced solely oligomers. Surprisingly, the use of sulphuric acid resulted in a [2 + 2] macrocycle free of any by-products. This adduct is stable on its own through internal hydrogen bonding. Dominant formation of this macrocycle was due to a preference for tetrahedral anions as exemplified by strong binding interactions with HSO_4^- and H_2PO_4^- .⁶⁸

1.8 Scope of the Thesis

This thesis examines the synthesis and interactions of a dynamic receptor based upon the isophthalamide skeletal structure. Pyridine dicarboxamide has shown to bind anions while installing a pre-organized binding cavity (Figure 1.4).^{19,20} The inclusion of a Schiff base moiety would create a site where reversible exchange can occur. There have been few examples in which a receptor binding cavity is pre-organized and created through the formation of Schiff bases. A semicarbazone unit would allow a more stabilized product to be formed while meeting the desired pre-organizational needs (Figure 1.21). The binding of this resulting receptor to various anionic species will be explored along with the effects of various TBA anion templates upon receptor formation.

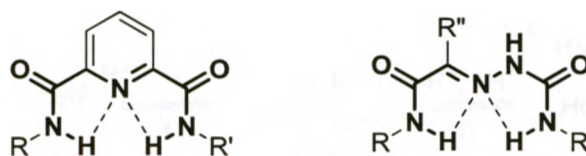


Figure 1.21 – Pyridine dicarboxamide (left) and dynamic receptor examined in this thesis (right).

Chapter 2

2.1 Introduction

2.1.1 Schiff Base

The reaction of an amine with an aldehyde or ketone to form an imine was first discovered by Schiff in 1864.⁶⁹ Traditionally this reaction is carried out with an azeotroping agent and an acid catalyst.⁷⁰ The reaction is generally first order in respect to the nitrogen and carbonyl compounds.⁷¹ In acidic conditions the attack on the carbonyl by an amine is the rate-determining step (step I in Figure 2.1). Though the carbonyl is protonated creating a better electrophilic site, the amine source can also be protonated thus hindering initial attack. Once attack has occurred, dehydration is fast as a result of available protons in the acidic environment.

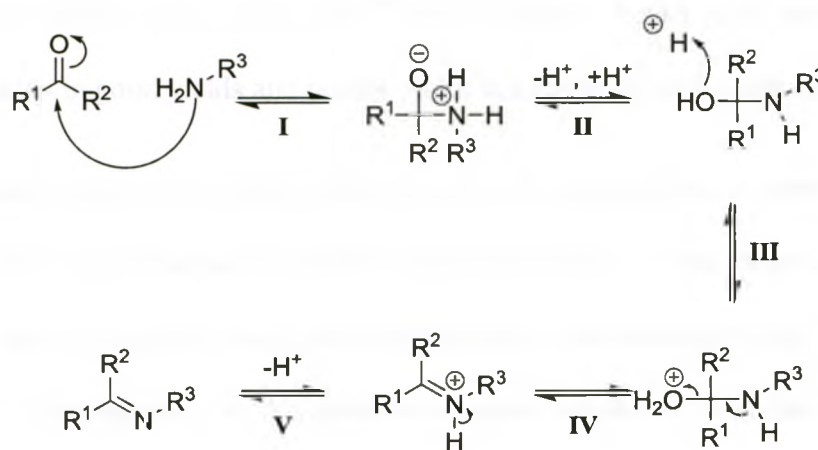


Figure 2.1 - General mechanism of imine formation.

However, in neutral or basic conditions, the dehydration of the carbinolamine intermediate is the rate-determining step (III and IV of Figure 2.1). In this situation, the

amine is free to attack the carbonyl but there is a reduced availability of protons to protonate the alcohol leading to dehydration and formation of the Schiff base.⁷² These properties are also observed when the amine source is a semicarbazide.⁷³

When amines react with aldehydes attached to primary or secondary aliphatic groups there is the possibility of aldol side reactions that can occur resulting in polymeric species. However when tertiary aliphatic or aromatic aldehydes are employed Schiff base formation occurs even without the removal of water. This attests to the reactivity of these aldehyde species in this reaction.

Higher temperatures and longer reaction times are needed when using aliphatic ketones. In these situations, acid catalysts and the removal of water is often necessary to obtain moderately-high yields. The reaction of aromatic ketones is slower and the use of a Brønsted or Lewis acid is essential.⁷⁰ Use of dialkyl ketals with aromatic amines generally results in good yields and poorer yields are observed with aliphatic amines.

Young and co-workers studied the formation of a semicarbazone from pyruvamide and *N*-substituted pyruvamide in buffered aqueous solutions.⁷⁴ The presence of an amide provides an electron-withdrawing group that increases the electrophilicity of the ketone to attack by the semicarbazide. *N*-propylpyruvamide was shown to be less reactive than pyruvamide. *N,N*-dimethylpyruvamide was about 20 times less reactive than pyruvamide and 10 times less reactive than *N*-propylpyruvamide. These results were similar to that of Pino and co-workers where ethyl pyruvate displayed reactivities 20 times less than pyruvic acid.⁷⁵ An equilibrium was proposed that involved internal hydrogen bonding by pyruvamide during the formation of the carbinolamine (Figure 2.2).

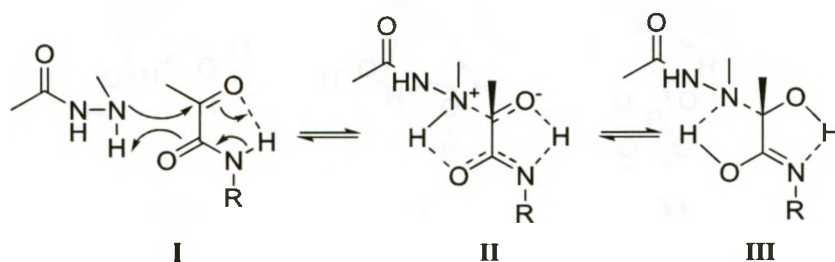


Figure 2.2 – Proposed intermediates towards carbinolamine formation.

The internal hydrogen bonding provided by pyruvamide aids during semicarbazide attack and results in a zwitterionic intermediate (**II**) which resolves to **III** (Figure 2.2). The lower reactivity of the *N,N*-alkylpyruvamide and ethyl pyruvates can be plausibly explained due to the lack of this internal hydrogen bonding. The formation of the carbinolamine intermediate is also accelerated in the presence of H_2PO_4^- and surprisingly HPO_4^{2-} . These two phosphate ions could potentially act in the protonation of the carbinolamine zwitterion (**II**). This would be a similar effect as that of water during fast proton transfers (Figure 2.3) and as such would be limited to the diffusion capabilities of the phosphate ions within the solvent to the reactive centres.

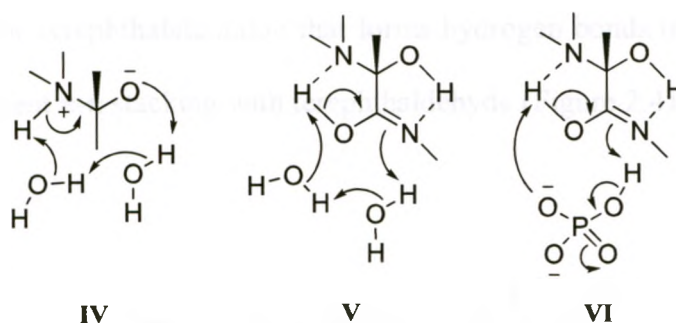


Figure 2.3 - Solvent and catalyst assisted proton transfers in carbinolamine formation.

The proton transfers in Figure 2.3 show for the generic attack on a ketone (IV), similar pathways being applied for the carbinolamine (V) and potentially a similar route for HPO_4^{2-} . In the uncatalyzed reaction, in the absence of phosphate ion, the rate is still considerably higher than that for ethyl pyruvate. The hydrogen bonding sequence described above illustrates the subtleties of the possibilities that the presence and lack of hydrogen bonding can provide.

2.1.2 Anion acceleration of Schiff base formation of pseudopeptidic macrocycles.

The use of hydrogen bonding and fast proton transfers was also exploited by Bru and co-workers in Schiff base formation in the synthesis of an anion receptor.⁷⁶ The condensation between a bis(amidoamine) and a dialdehyde was accelerated in the presence of a terephthalate dianion, whereas in the presence of other anions (chloride, acetate and benzoate as tetrabutylammonium salts) there were only minor increases in the rate of product formation observed. The two components are brought together, [2 + 2], in

the presence of the terephthalate anion that forms hydrogen bonds to the amides present and to a lesser extent π - π stacking with terephthalaldehyde (Figure 2.4).

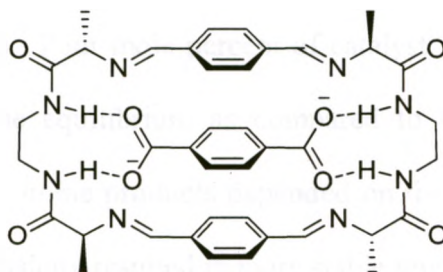


Figure 2.4 - Pseudopeptidic macrocycle binding terephthalate.

There is the possibility for not only the terephthalate to bring all of the subunits together, but to also act as a proton shuttle in the condensation process. The dianion would also hydrogen bond to the free amine and shuttle protons to the aldehyde during the reaction. This shuttling process holds true with the concept of acid-base catalysis on Schiff base formation. The final macrocycle would not only participate in hydrogen bonding with the terephthalate, but also in π - π stacking.

2.1.3 Lewis Acid catalyzed Schiff base exchange in non-aqueous conditions.

Lewis acids have accelerated the transimination of Schiff bases. Giuseppone and co-workers have observed this phenomenon with lanthanides.⁷⁷ As the radii of the lanthanide being used decreases the greater the acceleration observed and as such

scandium (III) was observed to be the best choice. Accelerations of the exchange process were dependent on the amount of catalyst present. The imine and amine coordinate with the scandium catalyst. The stronger coordinating or more basic the amine, the greater the interaction with the Lewis acid and as a result shifts the equilibrium distribution among the possible imine products. Four mole percent of catalyst was observed to be optimal with no influence upon the equilibrium as compared to the non-catalyzed reaction. Stability and distribution of imine products depended on the amine being used. Amines with higher reactivity and basicity resulted in more stable imines, as would be expected.

Scandium was compared with trifluoroacetic acid to evaluate the difference between Bronsted and Lewis acids. There were decreased reaction times with both reagents, but scandium displayed higher activity in terms of the initial rates.

2.1.4 Hydrazone containing anion receptors

The hydrazone motif has been employed in the design of other anion receptors. Gupta *et al* have synthesized a receptor that has a high affinity for acetate⁷⁸ (Figure 2.5). The receptor was formed from the condensation reaction of 2,4-dinitrophenylhydrazine and acetylacetone resulting in a compound with two hydrogen bonding sites. Wang and co-workers designed another acetate receptor.⁷⁹ This colorimetric receptor arises from 5-nitro-1,3-benzenedicarboxaldehyde being condensed with 4-nitrophenylhydrazine. In addition to acetate, binding of fluoride and dihydrogen phosphate was observed with each varying by an order of magnitude, while the other halides exhibited no detectable

binding. Wang proposes this receptor to contain four hydrogen bonding sites to bind anions via two N-H and two C-H hydrogen bond donors.

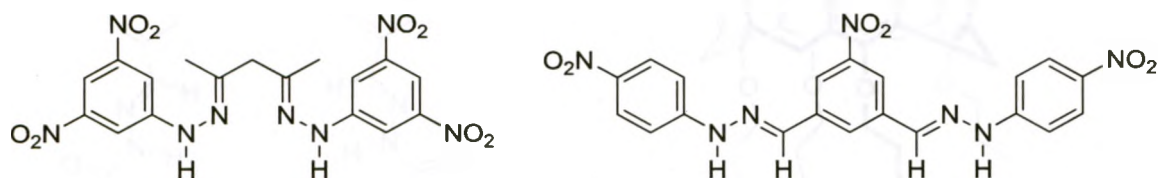


Figure 2.5 - Gupta's (left) and Wang's (right) hydrazone receptor.

Chawla and co-workers have used a semicarbazone formed from the addition of a semicarbazide to a calix[4]arene (Figure 2.6). In these structures there was anticipated to be a difference in anion selectivity depending on whether attachment was to the upper or lower rim of the calix[4]arene. When attached to the lower rim there is a selectivity for hydrogensulfate⁸⁰ ($4.5 \times 10^3 \text{ M}^{-1}$, CDCl_3), while attachment at the upper rim results in selectivity for dihydrogenphosphate⁸¹ (1890 M^{-1} , DMSO). In the former case, two semicarbazones were formed, while in the latter there were four semicarbazone units present.

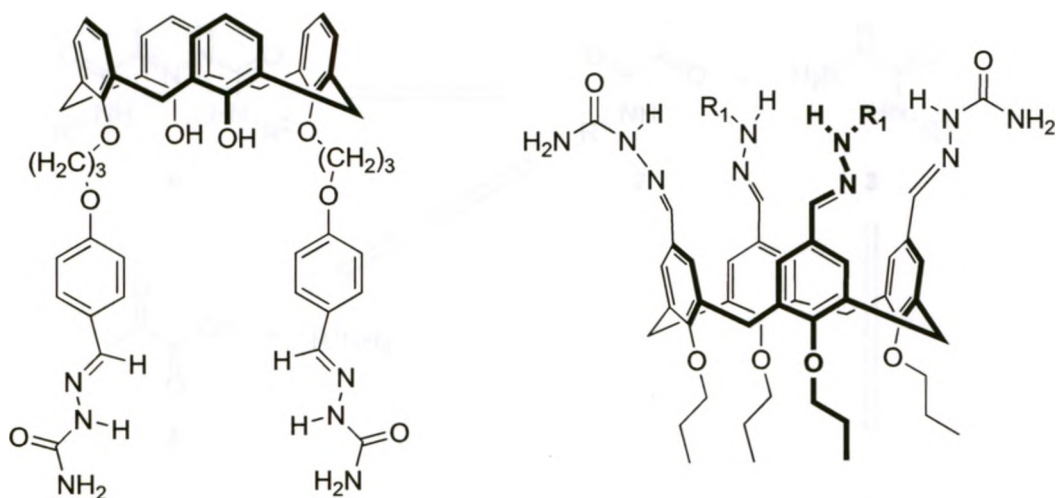


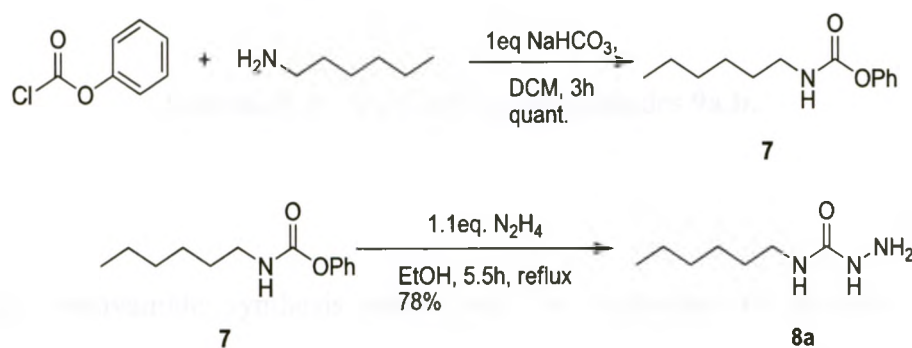
Figure 2.6 - Chawla's calix with a lower (left) and an upper (right) rim binding site.

2.1.5 Semicarbazone containing anion receptors

As mentioned in chapter one, a receptor was designed that will contain a hydrazone linkage while adopting a geometry similar to that of pyridine dicarboxamide. A semicarbazone motif allows for a dynamic linkage that will allow assembly and disassembly of the receptor, while also providing an amide source mimicking pyridine dicarboxamide. The design of this desired receptor derives from the condensation between a 4-substituted semicarbazide and that of a pyruvamide. The retro-synthetic route is shown in Figure 2.7.

2.2.1 Synthesis

As previously mentioned, synthesis of the desired receptors can be accomplished by the condensation between a 4-substituted semicarbazide and that of a pyruvamide. The semicarbazide can be synthesized from an active carbonyl species. In this case, phenyl chloroformate was added to *n*-hexylamine in dichloromethane (DCM) with sodium bicarbonate resulting in the quantitative formation of the carbamate. The carbamate species did not require any further purification and was used directly in the reaction with hydrazine to form 4-hexylsemicarbazide (Scheme 2.1).



Scheme 2.1 – Synthesis of semicarbazide **8a**.

The 4-hexylsemicarbazide was purified by flash column chromatography with 10% methanol in dichloromethane as eluent. The synthesis of 4-phenylsemicarbazide (**8b**) would prove to be slightly more difficult due to the formation of a bisurea complex

as the major product. As a result of this, and its commercial availability **8b** was purchased.

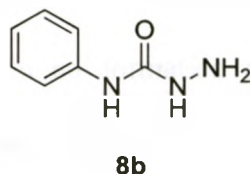


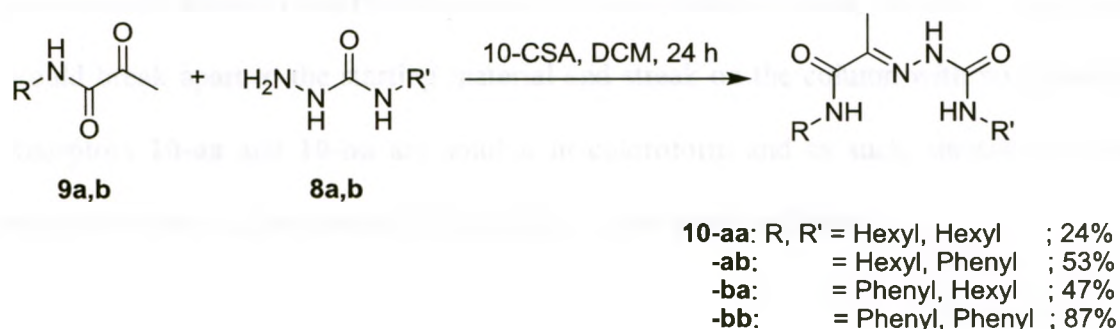
Figure 2.8 - Structure of semicarbazide **8b**



Scheme 2.2 – Synthesis of pyruvamides **9a,b**.

The pyruvamide synthesis starts with the formation of pyruvoyl chloride, followed by the addition of this to a solution containing the amine of choice with sodium bicarbonate (Scheme 2.2). Care is needed in this process as the pyruvoyl chloride possesses a low boiling point and, as such, any excess or un-reacted oxalyl chloride is very difficult to remove. The moderately low yields of 38% and 48% for the hexyl- and phenyl- derivatives respectively, are reflective of this complication. In both cases, the hexyl- and phenylpyruvamide, purification was carried out via flash column chromatography using hexanes/ethylacetate as eluent. In all cases, the bisamide from the reaction between the amine and oxalyl chloride was observed.

Once both fragments were obtained, the condensation between them was carried forward to the synthesis of our desired receptors. A classical approach in performing a condensation is refluxing the reagents in toluene with a Dean-Stark apparatus. Unfortunately, this method resulted in no formation of the desired products. Other approaches used in literature (including refluxing in methanol), were unsuccessful and returned only starting material. Knowledge gained from other attempts to perform the condensation reaction on similar compounds discussed later in this thesis led to the use of 10-camphorsulfonic acid as the method of choice (Scheme 2.3).



Scheme 2.3 - Synthesis of condensed semicarbazone receptors.

In cases where 4-phenylsemicarbazide was used as one of the starting reagents, the condensed products eventually precipitated out of solution after cooling and were filtered off. The phenylamido-phenylsemicarbazone (**10-bb**) resulted in a white solid with a yield of 87%. The hexylamido-phenylsemicarbazone (**10-ab**) required additional mixing and filtering as starting material was observed in the initial precipitate. These starting reagents are easily soluble in chloroform, while the receptor is insoluble allowing

reasonably facile purification to give a 53% yield. Because these two receptors, **10-bb** and **10-ab**, are insoluble in chloroform, anion binding studies could not be performed. The purification of the hexylamido-hexylsemicarbazone (**10-aa**) and phenylamido-hexylsemicarbazone (**10-ba**) required flash column chromatography with chloroform affording 24% and 47% yields, respectively. However the silica used needed to be pre-treated with 5% triethylamine-eluent. Any remaining starting material or other unwanted material would elute first through the column with some condensed product. As a result, reduced yields were observed due to loss of material in these early fractions of purification. When an insufficient amount of triethylamine is used, the condensed product would break apart to the starting material and streak on the column with no separation. Receptors **10-aa** and **10-ba** are soluble in chloroform and as such, titrations of these receptors with various tetrabutylammonium anions were performed.

2.2.2 Titrations with semicarbazone receptors

The isolated pure receptors (**10-aa**, **10-ba**) could now be tested for their affinity for binding various anions. In case of condensed products **10-ab** & **10-bb** that arose from the condensation with 4-phenylsemicarbazide, binding studies could not be performed due to insolubility in chloroform. One interesting note of all these receptors is that even though there is the possibility of internal hydrogen bonding to change the binding cavity, the desired open framework similar to that of pyridine dicarboxamide was observed as the predominant form (Figure 2.9).

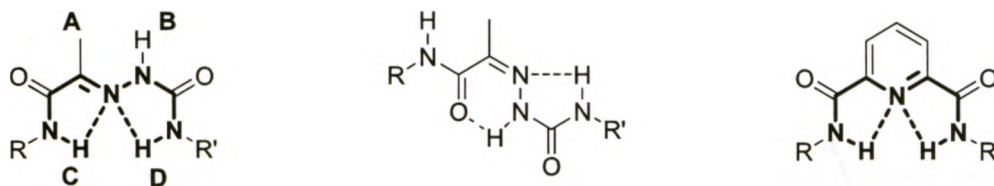


Figure 2.9 - Semicarbazone receptor with desired binding conformation (left), alternate binding conformation (middle) and pyridine dicarboxamide analogue (right).

In the case of 10-ba, proton **C** correlated with phenyl carbons as seen from ^1H HMBC, while proton **D** correlated with the methylene carbons of the alkyl chain. The ^1H ROESY spectrum (Figure 2.10) shows correlations between the methyl protons (**A**, $\delta = 2.11$ ppm) and the N-H ($\delta = 9.26$ ppm), labelled **B** as shown in Figure 2.9. This meant that proton **B** and those of **A** are within a close vicinity of each other. There are no correlations observed among the N-H proton with a chemical shift of 8.84 ppm (**C** in Figure 2.9) and that of the methyl **A** ($\delta = 2.11$ ppm) resonances. This meant that the alternate binding conformation was not present.

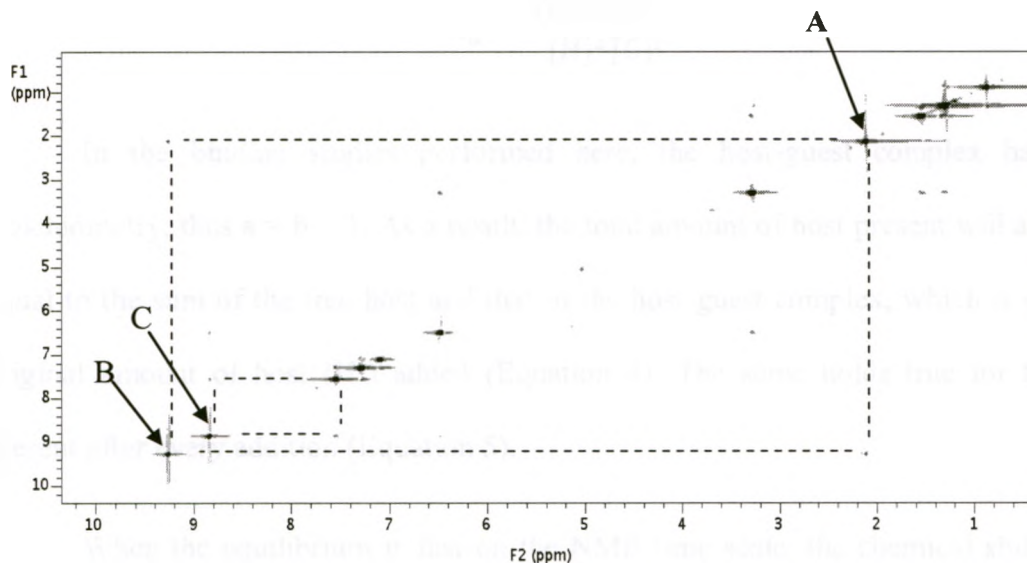
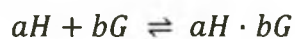


Figure 2.10 - ROESY ^1H NMR of Phenylamido-hexylsemicarboxide **10-ba**.

The association constants were determined through the use of ^1H NMR spectroscopy. The chemical shifts of a proton on a compound can represent the type of environment that the molecule resides in. When a binding study is carried out between a host (H) and Guest (G) changes in the chemical shifts of the host are observed. The host and guest will equilibrate to the formation of a host-guest (H·G) complex (Equation 1) with stoichiometric coefficients a,b.

Equation 1



The association constant will then appear as shown in Equation 2 .

Equation 2

$$K_a = \frac{[aH \cdot bG]}{[H]^a [G]^b}$$

In the binding studies performed here, the host-guest complex has a 1:1 stoichiometry, thus $a = b = 1$. As a result, the total amount of host present will always be equal to the sum of the free host and that of the host-guest complex, which is equal the original amount of host (H_o) added (Equation 4). The same holds true for the guest present after every addition (Equation 5).

When the equilibrium is fast on the NMR time scale, the chemical shifts of the protons of the compound in question will appear (Figure 2.11) as a weighted average (Equation 3) of the free host and the host-guest bound complex.

Equation 3

$$\delta_{obs} = \frac{H}{H_o} \delta_H + \frac{H \cdot G}{H_o} \delta_{H \cdot G}$$

Equation 4

$$[H_o] = [H] + [H \cdot G]$$

Equation 5

$$[G_o] = [G] + [H \cdot G]$$

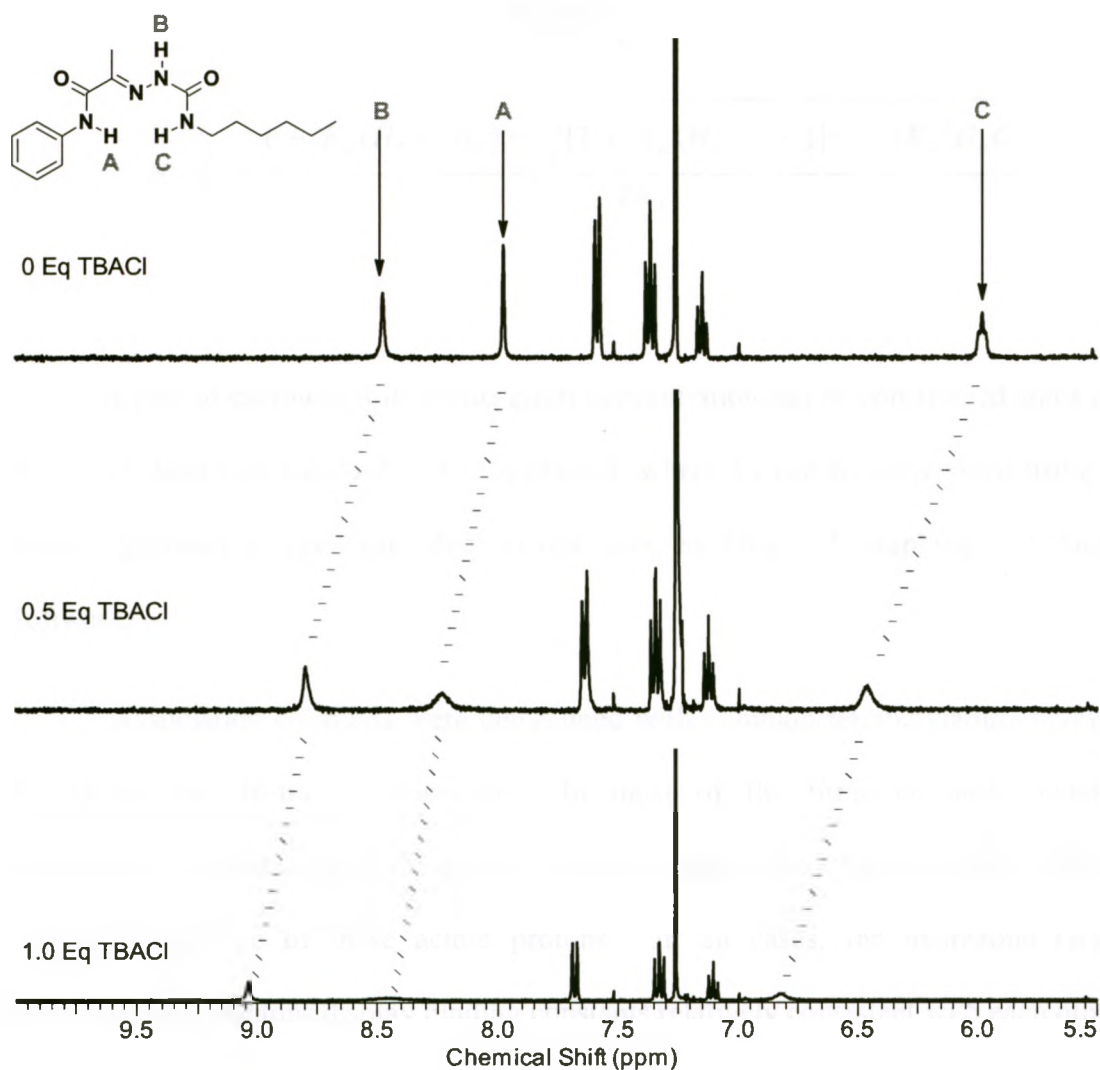


Figure 2.11 – Example of the change in chemical shift upon host-guest (**10-ba** TBACl) binding.

Equation 4 and Equation 5 can be substituted into Equation 2 and expanded to form a quadratic equation where the only unknown values are $[H \cdot G]$ and K_a while $[H_0]$ and $[G_0]$ are known. The quadratic can be solved for $[H \cdot G]$ (Equation 6), which is needed in Equation 3, while $[H]$ can be replaced from the rearrangement of Equation 4.

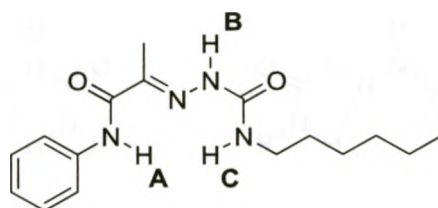
Equation 6

$$H \cdot G = \frac{1 + K_a(H_o + G_o) - \sqrt{[1 + K_a(H_o + G_o)]^2 - 4K_a^2H_oG_o}}{2K_a}$$

A plot of chemical shift versus guest concentration can be constructed and a curve of best fit determined according to Equation 3, where K_a can be determined using non-linear regression analysis provided, in our case, by Origin 7 Graphing and Analysis Software.

Association constants were determined with common tetrabutylammonium salts for **10-aa** and **10-ba** in chloroform. In most of the titrations with acetate or dihydrogenphosphate anions, the amide protons disappeared soon after addition. This is a result of exchange of these acidic protons. In all cases, the hydrazone (**B**) and hexylamide (**C**) protons display binding constants relatively consistent with each other.

As this molecule is not completely rigid, and contains three possible sites for hydrogen bonding, there are at least two different anion binding conformations that it can assume. One conformation would be the desired pyridine dicarboxamide-like binding cavity while another resembles a urea-like binding site (Figure 2.12). The urea motif has commonly been employed in the design of receptors for binding halides and carboxylates.³

Table 2 - Association constants of **10-ba** with various TBA salts in CDCl₃ at 298K.

TBA Salt	A		B		C	
	K_a (Lmol ⁻¹)	ΔG (kJ mol ⁻¹)	K_a (Lmol ⁻¹)	ΔG (kJ mol ⁻¹)	K_a (Lmol ⁻¹)	ΔG (kJ mol ⁻¹)
Cl ⁻	150	-12.5	810	-16.6	990	-17.1
Br ⁻	20	-7.6	40	-9.1	40	-9.2
I ⁻	N.C.	N.D.	N.C.	N.D.	N.C.	N.D.
HSO ₄ ⁻	360	-14.6	80	-10.8	80	-10.9
TsO ⁻	30	-8.6	50	-9.6	60	-10.0
AcO ⁻	N.D. ^b	N.D. ^b	260	-13.8	240	-13.6
H ₂ PO ₄ ⁻	N.D. ^b	N.D. ^b	190	-13.0	N.D. ^b	N.D. ^b

- Note: Association constant with corresponding proton in bold. N.C. = no change, no changes in chemical shift were observed. N.D. = Not Determined. ^b) Insufficient number of data points. Amide protons undergo fast exchange rendering them undetectable under the conditions of the experiment.

Each conformation cannot be isolated and have their respective binding values determined as there are numerous equilibria occurring between each conformation. The general association of the molecule and an anion can be discussed qualitatively. Though the binding values observed in **10-ba** are significantly lower than isophthalamide, they are approximately lower than that reported for diphenylpyridine dicarboxamide (Table 1).¹⁹

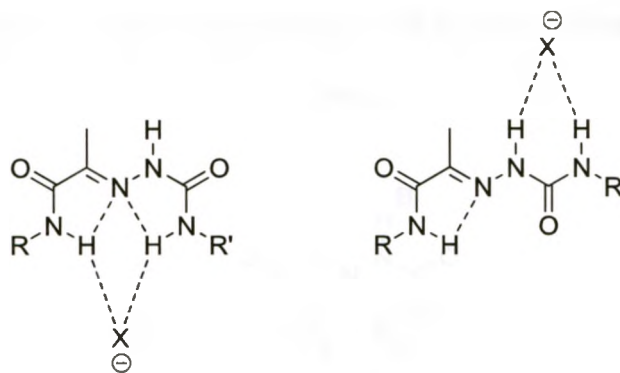
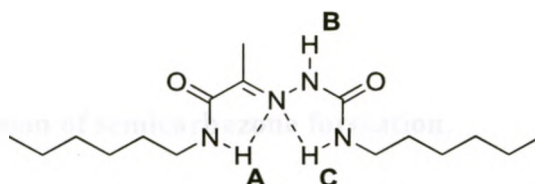


Figure 2.12 – Two possible conformations of semicarbazone receptors **10** with anions – Isophthalamide-like (left) and Urea-like (right) conformations.

However **10-ba** contains a less acidic hexyl amide, which would result in lower binding values. Though the titration of diphenylpyridine dicarboxamide is performed in CD_2Cl_2 , these values should still be comparable due to similarities between chloroform and dichloromethane. The preference for binding of chloride and acetate is common to all three of these receptors.

Dihexyl-semicarbazone receptor **10-aa** exhibits binding values that are relatively consistent among protons **A**, **B**, and **C** (Table 3). Interactions are observed between the receptor and all of the anions tested, though these association values are much reduced in magnitude compared to **10-ba**. One hydrogen bond donor site of **10-aa** is less acidic and thus weaker than **10-ba**.

Table 3 - Association constants determined for **10-aa** with various TBA salts in CDCl₃ at 298K.



TBA Salt	A		B		C	
	K_a (Lmol ⁻¹)	ΔG (kJ mol ⁻¹)	K_a (Lmol ⁻¹)	ΔG (kJ mol ⁻¹)	K_a (Lmol ⁻¹)	ΔG (kJ mol ⁻¹)
Cl ⁻	30	-8.4	20	-7.7	30	-8.0
Br ⁻	10	-6.6	20	-7.7	10	-6.6
HSO ₄ ⁻	30	-8.5	290	-14.0	40	-8.9
TsO ⁻	20	-7.5	10	-6.1	20	-7.3
AcO ⁻	50	-9.7	50	-9.6	50	-9.6
H ₂ PO ₄ ⁻	80	-10.9	N.D.	N.D.	N.D.	N.D.

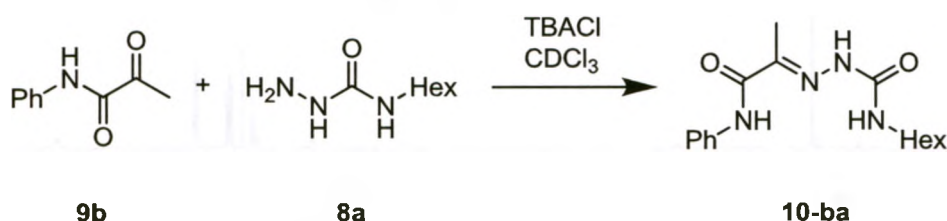
- Note: Association constant with corresponding proton underlined and in bold. N.D. = Not Determined – there were an insufficient number of data point available as the protons in question underwent fast exchange.

Chloride is the most strongly bound anion with receptor **10-ba**. In dynamic combinatorial chemistry, the goal is to possess a library of various components of similar energies that will form a potential array of products (receptors). The amplification of one receptor over another is dependent on the guest used to template the reaction. That is to say, the final product should possess a strong preference for binding for the guest in question. The fact that there is an association between a receptor and an anion shows that

there is a lower energy complex possible which only represents the thermodynamic preference of the receptor for the anion.

2.2.3 Anion acceleration of semicarbazone formation.

We were interested in whether anions would have an effect on the formation of the receptors (Scheme 2.4). The building blocks for receptor **10-ba** were reacted in the presence of TBACl as this combination displayed the highest association values from the titration studies described above.



Scheme 2.4 - Semicarbazone (**10-ba**) formation in the presence of chloride

Interestingly, there was an acceleration in formation of receptor **10-ba** depending on the concentration of TBACl used in the reaction. The initial rates were measured *via* ¹H NMR spectroscopy with various equivalents of TBACl and compared. Stock solutions were prepared from pre-dried reagents. The reagents, phenylpyruvamide, 4-hexylsemicarbazide and TBACl were azeotropically dried with toluene followed by placement under high vacuum for several hours. Kinetic runs were performed with starting reagents at a concentration in NMR tubes of approximately 0.02 M at a volume of 1 mL. Tetrabutylammonium chloride was added in various amounts ranging from zero

to four equivalents (Table 4). Tetrachloroethane was used as an internal standard to which integration values can be compared in the determination of species concentrations. Freshly prepared reagents were generally used prior to kinetic studies because older reagents possessed a reduced solubility in chloroform that would create significant inaccuracies in measurements of material being added. The presence of the starting pyruvamide and the resulting condensed receptor (**10-ba**) was monitored by observing the methyl group (A/B, Figure 2.13) that is adjacent to the reactive site.

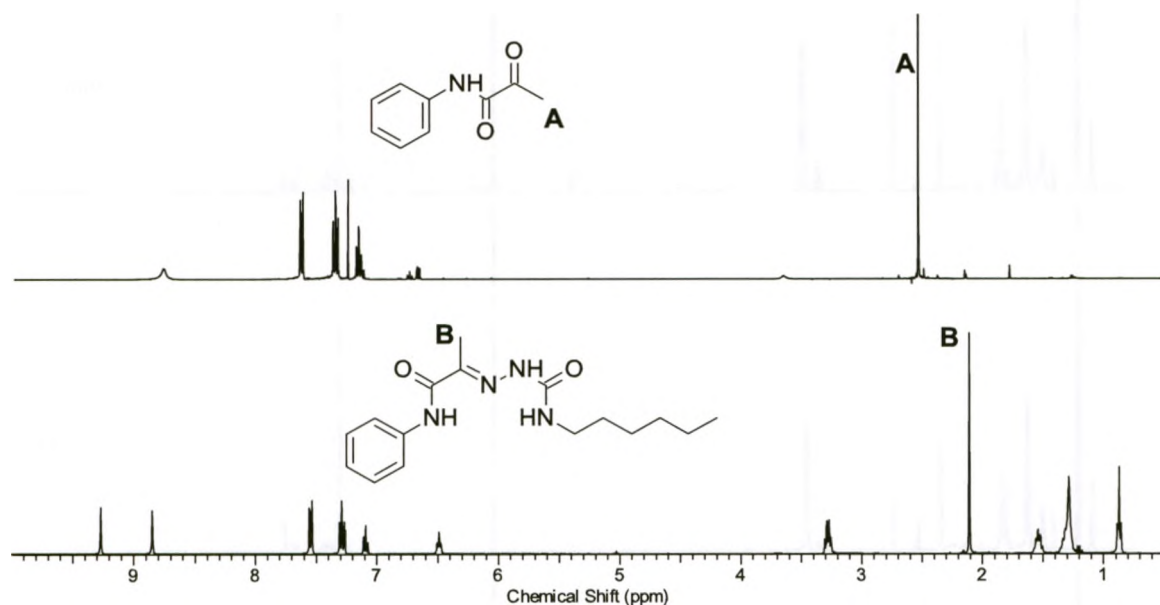


Figure 2.13 - ¹H NMR spectra in CDCl₃ of pure pyruvamide and condensed semicarbazone (**10-ba**).

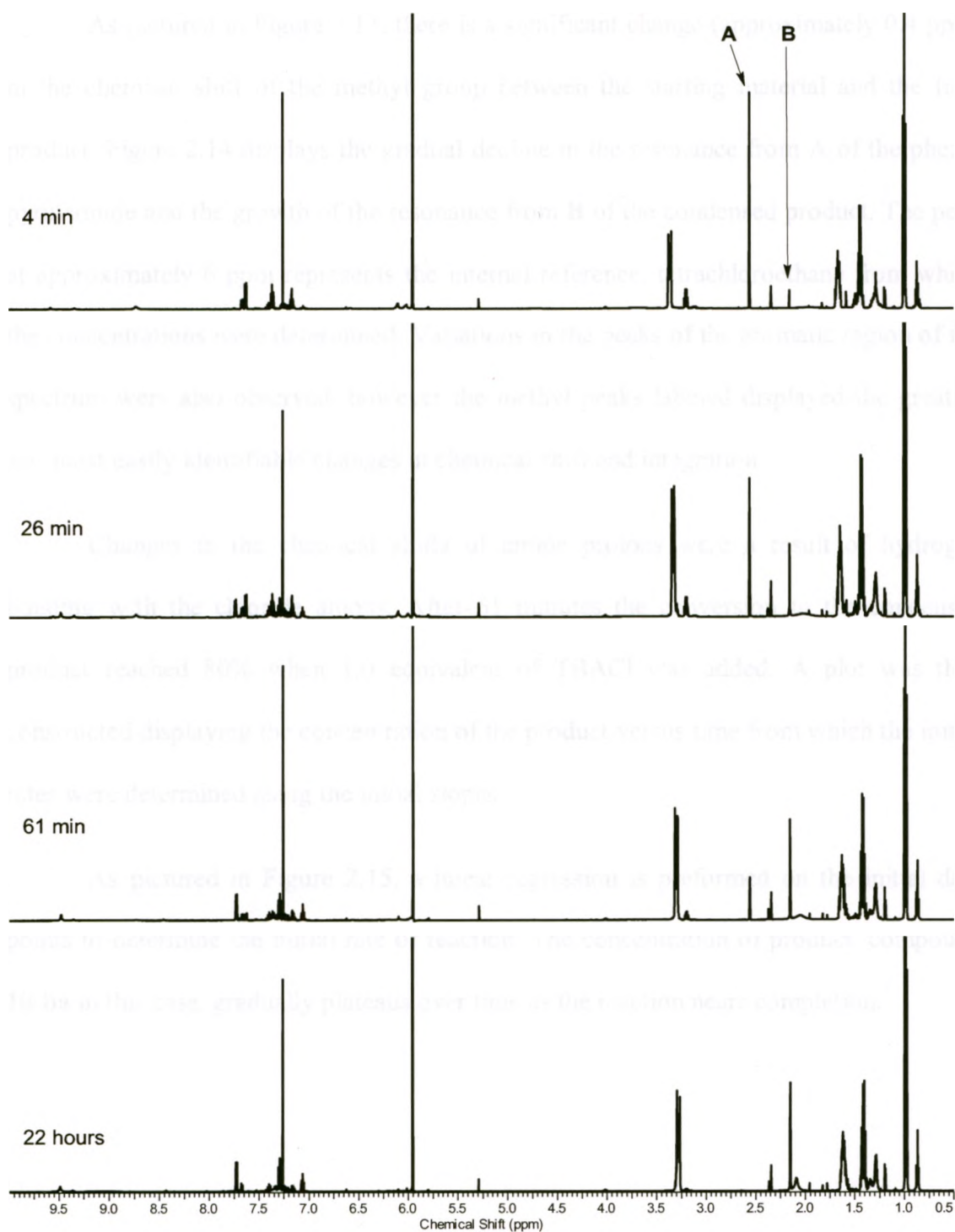


Figure 2.14 - Spectra of condensation between phenylpyruvamide (**9b**) and 4-hexylsemicarbazide (**8a**) in the presence of 1 equivalent of TBACl at various time intervals.

As pictured in Figure 2.13, there is a significant change (approximately 0.4 ppm) in the chemical shift of the methyl group between the starting material and the final product. Figure 2.14 displays the gradual decline in the resonance from **A** of the phenyl pyruvamide and the growth of the resonance from **B** of the condensed product. The peak at approximately 6 ppm represents the internal reference, tetrachloroethane from which the concentrations were determined. Variations in the peaks of the aromatic region of the spectrum were also observed, however the methyl peaks labeled displayed the greatest and most easily identifiable changes in chemical shift and integration.

Changes in the chemical shifts of amide protons were a result of hydrogen bonding with the chloride anions. After 61 minutes the conversion to the condensed product reached 80% when 1.0 equivalent of TBACl was added. A plot was then constructed displaying the concentration of the product versus time from which the initial rates were determined using the initial slopes.

As pictured in Figure 2.15, a linear regression is performed on the initial data points to determine the initial rate of reaction. The concentration of product, compound **10-ba** in this case, gradually plateaus over time as the reaction nears completion.

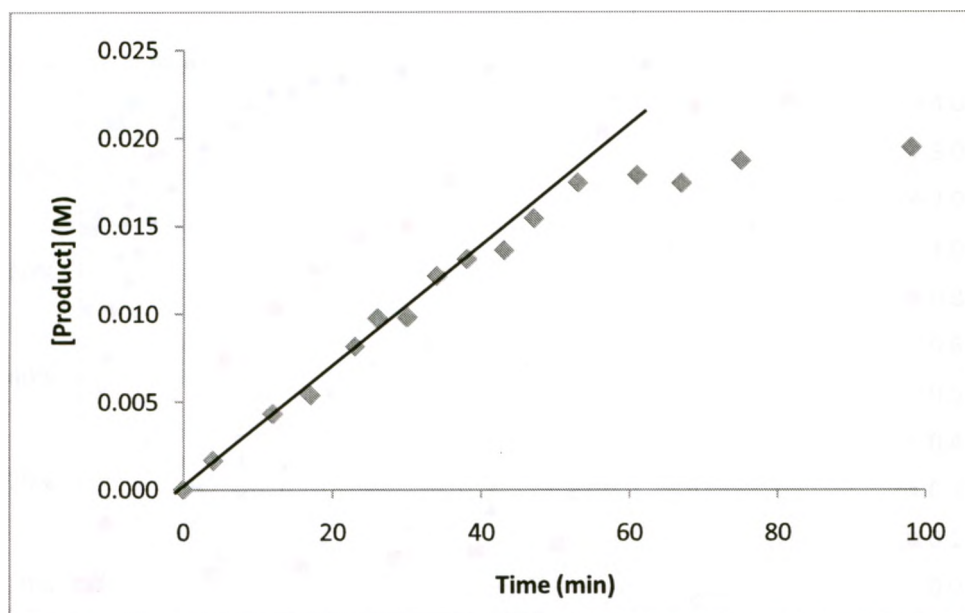


Figure 2.15 - Concentration of product from condensation reaction between phenylpyruvamide (20 mM) and 4-hexylsemicarbazide (20 mM) with 1 equivalent of TBACl over time with a line representing the best fit for the first eight points.

In cases where three or more equivalents of TBACl were used, product formation is complete within an hour (Figure 2.16). When less than half an equivalent was added, reaction completion is not achieved until more than twenty hours of reaction time has elapsed. A control reaction without any added TBACl, required more than three days to pass the half-way point (Figure 2.17). After this time, the concentrations of reacting species began to change appreciably as a result of solvent evaporation.

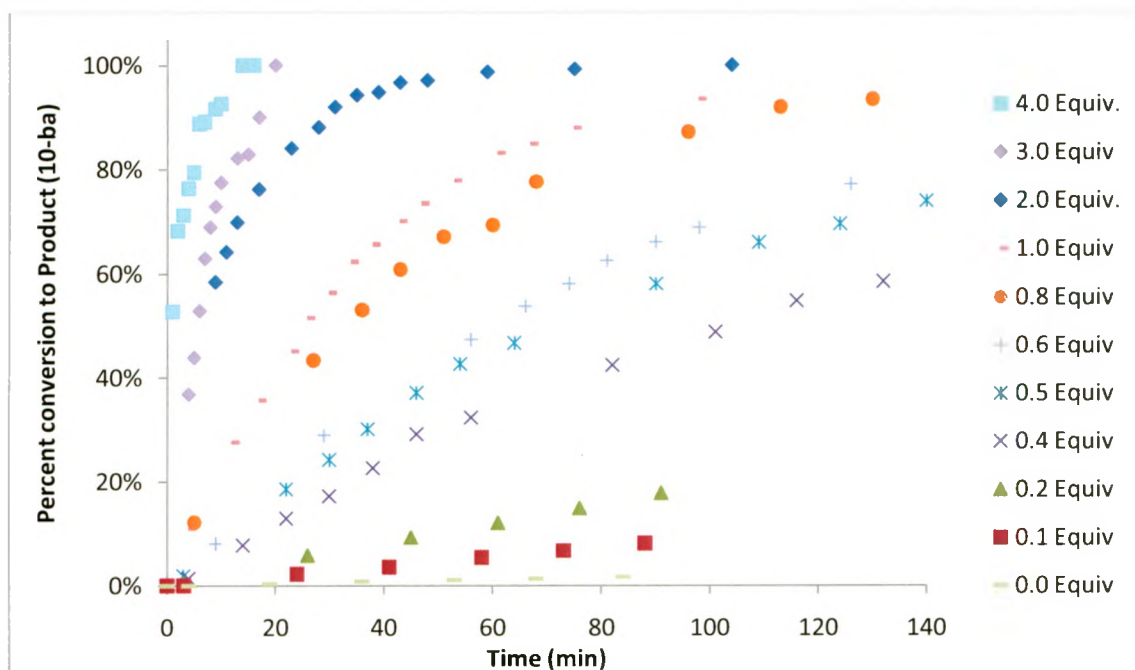


Figure 2.16 - Percent of receptor **10-ba** formation over initial 140 minutes with 0 – 4 equivalents of TBACl added.

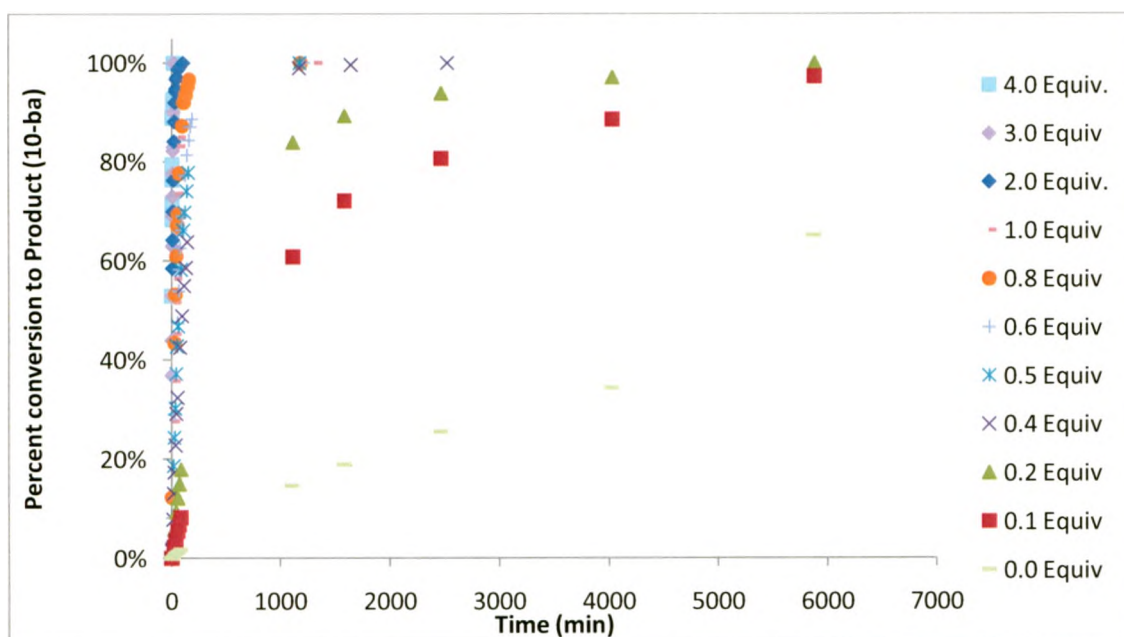


Figure 2.17 - Percent formation of receptor **10-ba** over time with 0 – 4 equivalents of TBACl added.

Table 4 – Increase in initial rates of formation of **10-ba** in the presence of different amounts of TBACl.

Eq. TBACl	Initial Rate (M / min)	Rate X Eq./Rate 0 Eq.
0	1.3E-06	1
0.1	9.1E-06	7
0.2	3.4E-05	25
0.4	9.4E-05	69
0.5	1.4E-04	105
0.6	1.5E-04	111
0.8	2.9E-04	216
1	3.1E-04	234
2	1.1E-03	836
3	1.6E-03	1241
4	5.1E-03	3766

The initial rates at the various TBACl concentrations were compared to the initial rate when TBACl was absent. The ratios of the accelerated rates compared to the control are expressed in the third column of Table 4. There is a significant change in the initial rates of reaction for product formation with respect to the amount of TBACl added. The initial rate data can be used in determining the order of chloride in the reaction. A plot can be made of the natural log of the rates versus the natural log of the concentration of the respective rates. The slope of this plot represents the reaction order of the species being graphed (Figure 2.18).

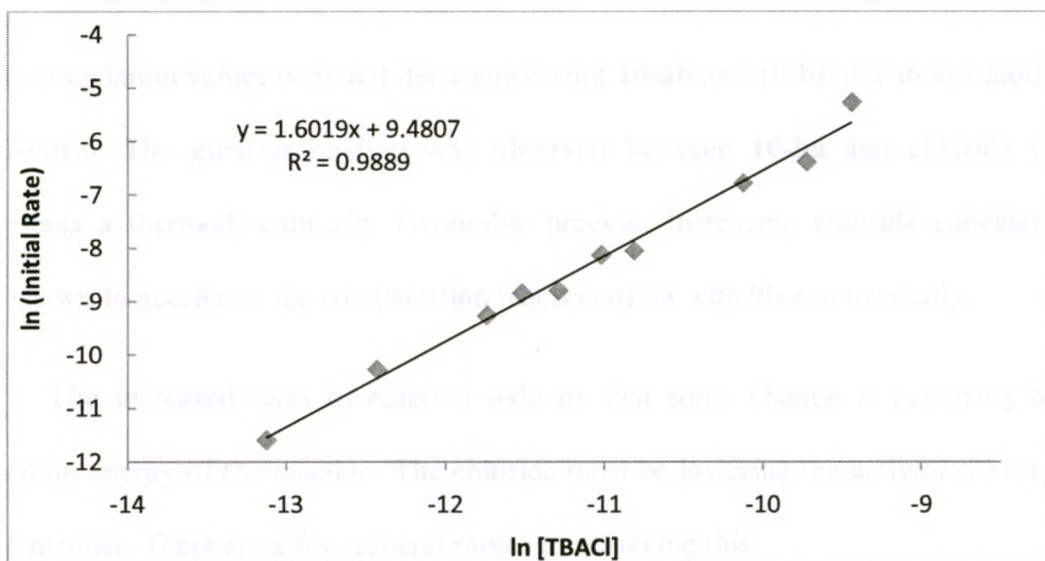


Figure 2.18 - Plot of natural logs of initial rates versus concentrations of TBACl.

The slope of the plot shown in Figure 2.18 is 1.60, which is very close to 1.5. TBACl has a pseudo-one and a half order participation in the condensation reaction. The rate of reaction is directly related to the concentration of chloride present. It is possible that the chloride hydrogen bonds with the various components or intermediates through the condensation reaction. The water content of CDCl_3 used was determined to be less than 5 ppm and therefore unlikely to impact the condensation process.

Using hexylpyruvamide (**9a**) instead of phenylpyruvamide (**9b**) with **8a** in the absence of TBACl resulted in no reaction. However when one equivalent of TBACl was present receptor **10-aa** was observed with an initial rate of reaction of $8.6 \times 10^{-4} \text{ M min}^{-1}$.

2.2.4 Summary and Conclusions

Receptors **10-aa** and **10-ba** interact with various anions as tetrabutylammonium salts. Association values were not determined with **10-ab** and **10-bb** due to insolubility in chloroform. The greatest binding was observed between **10-ba** and chloride which represents a thermodynamically favourable process. Increasing chloride concentration was shown to accelerate the condensation reaction of **8a** with **9b** exponentially.

The increased rates of reaction indicate that some change is occurring to the activation energy of the reaction. The chloride must be lowering the activation energy in some manner. There are a few general routes to achieving this:

i) The reactants are brought together.

The TBACl must be interacting non-covalently with the components of the reaction. Titrations performed with TBACl and phenylpyruvamide (**9b**) displayed no correlation. While 4-hexylsemicarbazide (**8a**) and TBACl presented a correlation of 38 M^{-1} as would be expected with a urea motif in the presence of an anion. This association value for a two species complex is fairly low. The association value of this complex with a third component would be significantly smaller. It is unlikely for TBACl to be bringing the components together, but rather interacting with a reaction intermediate.

ii) Chloride aids in the positioning of the transition state conformation.

Similarly to Young and co-workers, internal hydrogen bonding of the pyruvamide likely increases the electrophilicity of the carbonyl carbon to nucleophilic attack. This is best exemplified by the poor hydrogen bond donor, less acidic hexylpyruvamide (**9a**) resulting in no product formation in the absence of TBACl. When TBACl is present with

9a and **8a** condensation does occur. However, product formation is observed with **9b** + **8a** in the absence of TBACl. Chloride, a strong hydrogen bond acceptor, must be interacting with some transition state intermediate through hydrogen bonding. Sequential removal of the hydrogen bonding sites would provide insight into what role they play with TBACl in the acceleration of semicarbazone formation which shall be discussed in the following chapter.

iii) Chloride provides an alternative in the mechanism.

Chloride is a strong hydrogen bond acceptor and is likely not basic enough to act as a brønsted base. Though, it may be providing an alternative mechanism through hydrogen bonding. Removal of hydrogen bonding sites as mentioned above will also test the role that chloride has and the potential for an alternative mechanism. However, providing an alternate mechanism can also be tested by replacing chloride with some other anion to determine whether the mechanism is chloride dependant. This shall be discussed further in the following chapter of this thesis.

2.3 Experimental

General Considerations

All Reactions were performed under inert atmosphere with dry solvents unless otherwise stated. All chemical reagents were purchased from Sigma Aldrich or Alfa Aesar. Pure silica gel (230 – 400 mesh) purchased from Silicycle Chemical Division Inc. was used for flash chromatography. ^1H (400 MHz) and ^{13}C (100 MHz) NMR were

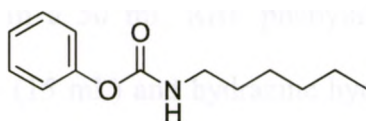
collected using a Varian Mercury 400 MHz instrument, peak assignment are reported as follows: chemical shifts (δ , in ppm) are referenced to the proton residual in CDCl₃ and DMSO-*d*₆, integration, multiplicity.

¹H NMR Titrations in CDCl₃ were performed on a Varian Inova 400 MHz instrument. Deuterated chloroform was used as solvent and performed with a host concentration of 5×10^{-3} M. Appropriate aliquotes of guest (containing host as background) are added using Hamilton Gastight microliter syringes. Titration data from observations of the appropriate protons (amide protons) were curve fitted with Origin Scientific Graphing Software to match a 1:1 host:guest association model.

Kinetic experiments were performed with CDCl₃, which was washed with water (2 x 50 mL), stirred in potassium carbonate for 30 minutes, followed by distillation over calcium chloride before being stored over pre-activated molecular sieves. Water content was determined to be less than 5 ppm with the use of Karl Fischer 684 KF Coloumeter apparatus. Stock solutions of reagents were prepared by azeotropically removing any water present in pre-weighed RBF with septa followed by placement under high vacuum (~1.5 torr) for up to 4 hours before being backfilled with nitrogen. Appropriate masses of reagents and volumes of CDCl₃ were used such that the concentration of the stock solutions was made to add approximately 100 μ L of material to attain a 1.0 equivalent of 0.02 M NMR tube concentration. After drying of reagents and addition of CDCl₃ to create stock solutions, the volumes for addition to NMR tubes were recalculated appropriately. NMR tubes were closed with Teflon caps and wrapped with parafilm. NMR spectra were taken on a Varian Inova 600 MHz instrument. A ¹H NMR spectrum was taken of NMR tube solutions prior to the addition of the semicarbazide or amine

(time zero). After addition of the semicarbazide, spectra were taken and the corresponding reaction time calculated from the time of acquisition completion of the spectra. The growth and loss of ^1H NMR were monitored of the methyl peaks of the starting pyruvamide and newly formed receptor. Non-deuterated tetrachloroethane ($5\ \mu\text{L}$) was used as an internal reference for integration and concentration determination. Linear regression analysis was performed on the initial concentrations of product formation to determine initial rates.

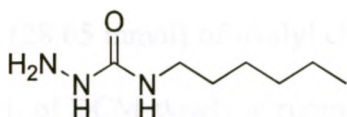
Phenyl hexylcarbamate – (7)



In a 250 mL RBF, 3.845 g (45.77 mmol) of sodium bicarbonate, 6 mL (45.42 mmol) of hexylamine was stirred in 50 mL DCM and cooled in an ice bath. To this solution was added 5.75 mL (45.69 mmol) of phenylchloroformate in 20 mL DCM dropwise. The reaction was then left to stir for 2 hours at which time, water was added (100 mL) and the organics extracted with DCM (3 x 60 mL). The combined organics were then washed with 1 M sodium bicarbonate (1 x 100 mL), 5% HCl (1 x 100 mL), water (2 x 100 mL) followed by drying and evaporation of volatiles yielding a white solid 9.8482 g (98%) requiring no further purification. ^1H NMR values obtained match that of Minkkila and co-workers.⁸²

^1H NMR (CDCl_3 , δ): 7.35 (t, $J = 7.6$ Hz, 2 H), 7.19 (t, $J = 6.8$ Hz, 1 H), 7.12 (d, $J = 8.4$ Hz, 2 H), 3.26 (m, 2 H), 5.06 (s, 1 H), 1.58 (m, 2 H), 1.58 (m, 2 H), 1.32 (m, 6 H), 0.90 (t, $J = 6.6$ Hz, 3 H).

***N*-hexylhydrazinecarboxamide – (8a)**

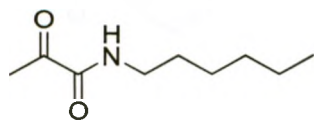


In a 50 mL RBF phenylhexylcarbamate, **7** (0.885 g, 4.00 mmol) in absolute ethanol (15 mL) and hydrazine hydrate (0.2 mL, 4.095 mmol) were heated under reflux for 5.5 hours. Upon completion of the reaction, water (20 mL) was added followed by extraction of the organics with DCM (2 x 20 mL). The combined organics were then dried and the volatiles evaporated. The pure product was isolated using flash column chromatography (FCC) (9:1 DCM:MeOH) giving a white solid, 0.452 g, 78%.

^1H NMR (CDCl_3 , δ): 6.37 (s, 1 H), 6.04 (s, 1 H), 3.64 (s, 2 H), 3.21 (m, 2 H), 1.50 (m, 2 H), 1.29 (m, 6 H), 0.87 (t, $J = 6.8$ Hz, 3H).

^{13}C NMR (CDCl_3 , δ): 160.4, 109.7, 39.6, 31.5, 30.2, 26.5, 22.5, 13.9.

HRMS: calc for $\text{C}_7\text{H}_{17}\text{N}_3\text{O}$: 159.1372, found: 159.1365.

Hexylpyruvamide - (9a)

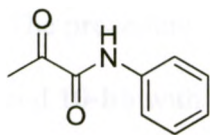
To a 50 mL RBF containing one drop of dimethylformamide, 15 mL of DCM and 2.5 mL (28.65 mmol) of oxalyl chloride was added 2 mL (28.65 mmole) of pyruvic acid in 10 mL of DCM slowly at room temperature. Upon completion of addition, the solution was stirred for three hours. The solution was then added dropwise to a second 250 mL RBF containing 2.486 g (29.59 mmole) sodium bicarbonate and 3.8 mL (28.77 mmole) of hexylamine in 50 mL DCM. After three hours, water (50 mL) was added and the organics extracted with DCM (3 x 50 ml). The combined organics were washed with water (1 x 100 mL), 5% HCl (1 x 75 mL), dried with magnesium sulfate, filtered and the volatiles evaporated. The product was isolated using FCC (7:3 hexanes:ethylacetate) yielding a white oil 1.869 g (38%).

^1H NMR (CDCl_3 , δ): 6.95 (s, 1 H), 3.28 (m, 2 H), 2.47 (s, 3 H), 1.53 (m, 2 H), 1.29 (m, 6 H), 0.87 (t, $J = 7.0$ Hz, 3 H).

^{13}C NMR (CDCl_3 , δ): 197.3, 160.0, 39.4, 31.4, 29.2, 26.5, 24.4, 22.5, 13.9.

HRMS: calc for $\text{C}_9\text{H}_{17}\text{NO}_2$: 171.1259, found: 171.1257.

Phenyl Pyruvamide – (9b)



To a 50 mL round bottom flask containing one drop of dimethylformamide, 10 mL of DCM and 0.93 mL (10.6 mmol) of oxalyl chloride was added 0.78 mL (11.2 mmole) of pyruvic acid in 10 mL of DCM slowly at room temperature. Upon completion of addition, the solution was left to stir for three hours. This solution was then added dropwise to a second 100 mL RBF containing 1.721 g (12.5 mmol) potassium carbonate and 1.2 mL (13.16 mmole) of aniline in 30 mL DCM. After three hours, water (50 mL) was added and the organics extracted with DCM (3 x 50 mL). The combined organics were washed with water (1 x 70 mL), 5% HCl (1 x 75 mL), dried with magnesium sulfate, filtered and the volatiles evaporated. The product was isolated using FCC (8:2 hexanes: ethylacetate) yielding a white-yellow solid 0.88 g (48%).

¹H NMR (CDCl₃, δ): 8.72 (s, 1 H), 7.65 (d, *J* = 8.8 Hz, 2 H), 7.38 (t, *J* = 7.4 Hz, 2 H), 7.18 (t, *J* = 7.4 Hz, 1 H), 2.58 (s, 3 H).

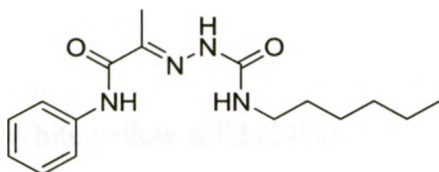
¹³C NMR (CDCl₃, δ): 153.5, 142.0, 129.2, 119.7, 114.5, 104.5, 28.2.

HRMS: calc for C₉H₉NO₂:163.0633, found: 163.0630

General method for condensation reactions

The procedure used for compound **10-ba**, was also applied for compounds, **10-aa**, **10-ab**, and **10-bb** with the appropriate pyruvamide and semicarbazide source.

Compound 10-ba - Phenylamidohexylsemicarbazone

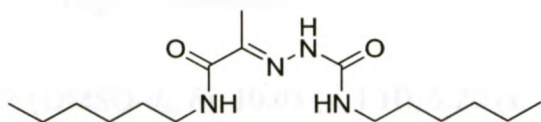


In a 50 ml RBF, 0.402 g (2.5 mmole) of phenyl pyruvamide, 0.382 g (2.46 mmole) of 4-Hexylsemicarbazide and 0.027 g (0.16 mmole) of 10-camphorsulfonic acid were stirred in 30 mL of DCM for 24 hours. Anhydrous sodium sulfate was then added and allowed to stir for five minutes before the reaction is filtered. The volatiles were removed from the filtrate. Purification was carried out using FCC (CHCl₃) with silica gel that was pre-treated with 5% triethylamine/CHCl₃ affording a white solid 0.347 g (47%).

¹H NMR (CDCl₃, δ): 9.26 (s, 1 H), 8.84 (s, 1 H), 7.55 (d, *J* = 8.2 Hz, 2 H), 7.29 (t, *J* = 7.8 Hz, 2 H), 7.09 (t, *J* = 7.4 Hz, 1 H), 6.48 (t, *J* = 5.9 Hz, 1 H), 3.27 (m, 2 H), 2.11 (s, 3 H), 1.54 (m, 2 H), 1.29 (m, 6 H), 0.87 (t, *J* = 6.6 Hz, 3 H).

¹³C NMR (CDCl₃, δ): 161.9, 155.5, 141.3, 137.3, 128.9, 124.4, 120.2, 39.9, 31.4, 30.0, 26.5, 22.5, 13.9, 10.1.

HRMS: calc for C₁₆H₂₄N₄O₂: 304.1899, found: 304.1908

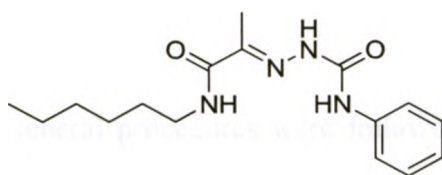
Compound 10-aa – Hexylamido Hexylsemicarbazone

White yellow solid (24%).

^1H NMR (CDCl_3 , δ): 8.94 (s, 1 H), 6.95 (t, $J = 5.9$ Hz, 1 H), 6.17 (t, $J = 5.9$ Hz, 1 H), 3.27 (m, 4 H), 2.08 (s, 3 H), 1.53 (m, 4 H), 1.28 (m, 12 H), 0.86 (m, 6 H).

^{13}C NMR (CDCl_3 , δ): 163.8, 155.5, 141.5, 39.9, 39.6, 31.4, 30.1, 29.6, 26.6, 26.5, 22.5, 13.9, 10.3.

HRMS: calc for $\text{C}_{16}\text{H}_{32}\text{N}_4\text{O}_2$: 312.2525, found: 312.2533

Compound 10-ab – Hexylamido Phenylsemicarbazone

The general procedure was followed, except a precipitate was observed prior to the addition of sodium sulfate. 20 mL of chloroform was added to the reaction vessel and then cooled at -30 °C for 18 hours. The precipitate was filtered off and then mixed with 6

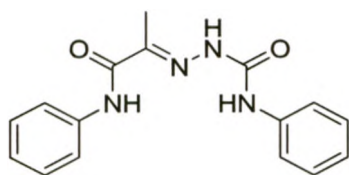
ml of chloroform before being cooled for additional 18 hours. The precipitate was then filtered yielding a white solid (54%).

^1H NMR (DMSO- d_6 , δ): 10.03 (s, 1 H), 9.22 (s, 1 H), 8.64 (t, $J = 5.9$ Hz, 1 H), 7.59 (d, $J = 8.6$ Hz, 2 H), 7.33 (t, $J = 7.8$ Hz, 2 H), 7.07 (t, $J = 7.4$ Hz, 1 H), 3.19 (m, 2 H), 2.01 (s, 3 H), 1.48 (m, 2 H), 1.26 (m, 6 H), 0.85 (t, $J = 6.6$ Hz, 3 H).

^{13}C NMR (DMSO- d_6 , δ): 163.6, 153.1, 141.0, 138.5, 128.5, 123.2, 120.9, 31.0, 29.3, 26.2, 22.1, 13.9, 11.1.

HRMS: calc for $\text{C}_{16}\text{H}_{24}\text{N}_4\text{O}_2$: 304.1899, found: 304.1900

Compound 10-bb – Phenylamido Phenylsemicarbazone



General procedures were followed except that a precipitate formed prior to the addition of sodium sulfate. As such, 20 ml of chloroform was added and the mixture was stored at -30 °C for 18 hours. The precipitate was then filtered off yielding off-white solid (87%).

^1H NMR (DMSO- d_6 , δ): 10.28 (s, 1 H), 10.21 (s, 1 H), 9.53 (s, 1 H), 7.75 (d, $J = 7.4$ Hz, 2 H), 7.66 (d, $J = 7.4$ Hz, 2 H), 7.36 (m, 4 H), 7.10 (m, 2 H), 2.12 (s, 3 H).

^{13}C NMR (DMSO- d_6 , δ): 162.3, 153.0, 140.9, 138.6, 138.4, 128.7, 128.6, 123.7, 123.0, 120.7, 120.5, 11.1.

HRMS: calc for $\text{C}_{16}\text{H}_{16}\text{N}_4\text{O}_2$: 296.1293, found: 296.1273

Chapter 3

3.1. Introduction

The condensed semicarbazone receptors, **10-aa** and **10-ba** (Figure 3.1), displayed an association with various anions in CDCl_3 , with chloride presenting the highest binding values. As these receptors contain a dynamic linkage, they are designed to be components in a dynamic combinatorial library. The goal of DCC is to construct a library of similar energy components that would preferentially form one product over another via self-assembly depending on the substrate/template employed.

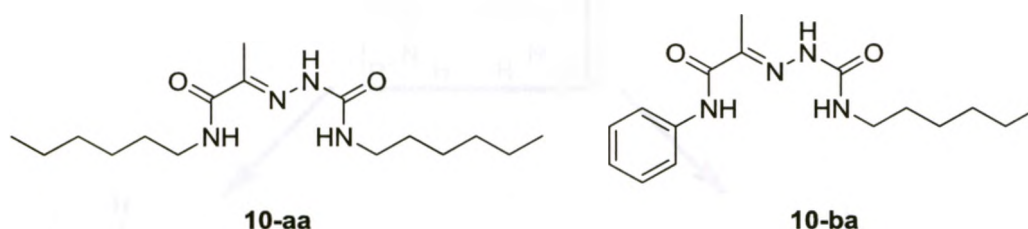


Figure 3.1 - Soluble condensed semicarbazone receptors

To this end, the formation of **10-ba** was tested in the presence of various concentrations of TBACl. Chloride had the strongest binding with the condensed receptor and as such was the substrate of choice. Acceleration in the rate of product formation was observed. It is likely that TBACl is interacting with the various species in solution through non-covalent interactions. Of all the possible non-covalent interactions, hydrogen bonding would appear to be the most probable due to the number of number of sites present and the general strength of these interactions. Hydrogen bonding with the 4-

hexylsemicarbazide was observed when a titration was performed with TBACl, but was not observed when the phenylpyruvamide was titrated with TBACl. Thus, the acceleration must be a result of lowering of a transition state likely due to stabilization of an intermediate involved in the rate determining step.

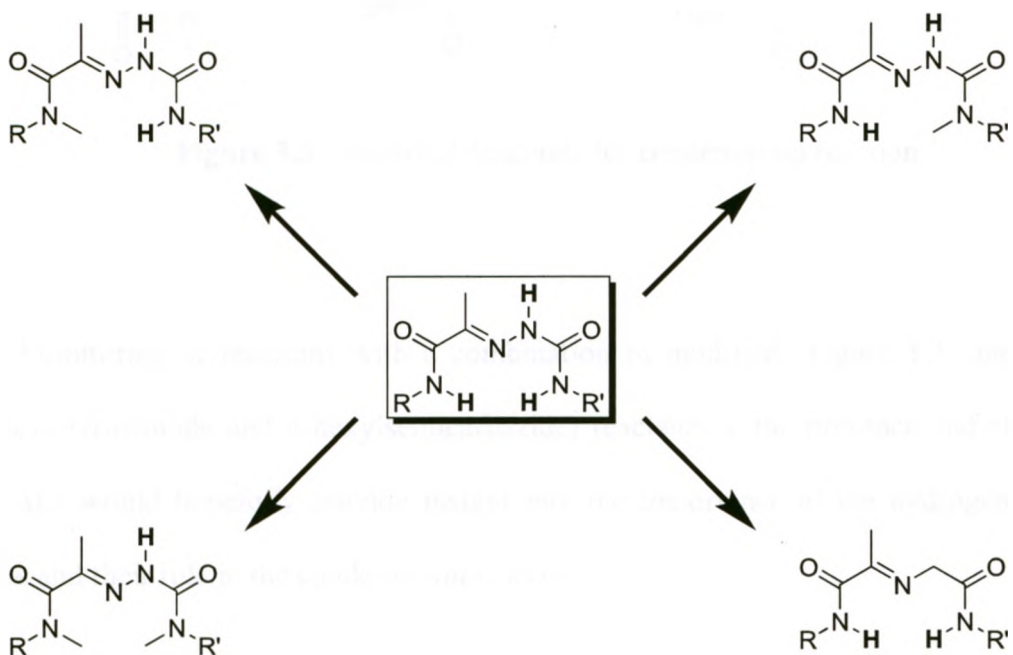


Figure 3.2 - Structure of modified semicarbazone receptors (periphery) and original receptor (centre).

As we cannot isolate the intermediates individually, the alternative course of action is to modify the possible site of interaction and observe the changes in reaction rate that occur as a result. The removal of the hydrogen bonding sites (in bold) was approached by

replacement of the hydrogen atoms in question with a methyl or methylene group as presented in the condensed structures of Figure 3.2. The methylated and methylene substituted starting reagents are pictured in Figure 3.3.

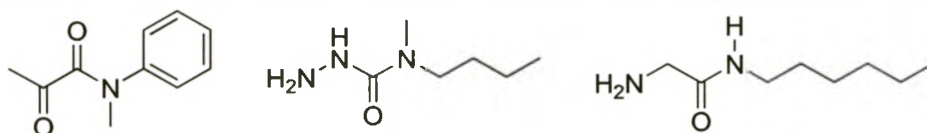


Figure 3.3 - Modified reactants for condensation reaction.

Monitoring of reactions with a combination of modified (Figure 3.3) and original (pheynpyruvamide and 4-hexylsemicarbazide) reactants in the presence and absence of TBACl would hopefully provide insight into the importance of the hydrogen bonding sites and their role in the condensation reaction.

The replacement of the N-H group with a methylene (Figure 3.2 lower right) would act in two ways. Not only would it test the importance of that hydrogen bonding site, but also test the application of TBACl in the acceleration of the condensation reaction towards primary amines and Schiff base formation. 2-amino-*N*-hexylacetamide which can be formed from the coupling of glycine with hexylamine was the choice of amine as it would allow the pyridine dicarboxamide skeletal structure to remain intact (Figure 3.4).

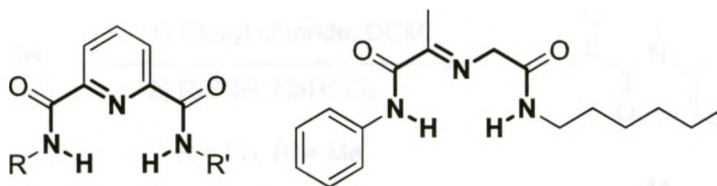


Figure 3.4 - Pyridine dicarboxamide (left) and Schiff base receptor **17** (right).

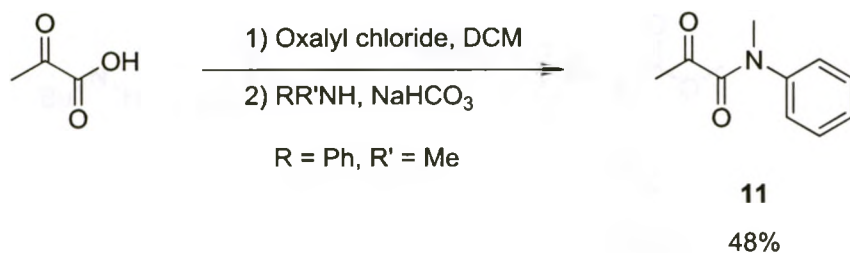
If hydrogen bonding is the main factor in the acceleration process, it might be possible that other anions can exhibit similar effects. The use of other TBA salts such as bromide, iodide, *p*-toluenesulfonate, hydrogensulfate, acetate, perchlorate, and hexafluorophosphate on the condensation rate of phenylpyruvamide with 4-hexylsemicarbazide was explored. Anions that are better hydrogen bond acceptors should result in increased reaction rates.

To explore these questions, the receptor components needed to be synthesized first.

3.2. Results and Discussion

3.2.1 Synthesis

N-Methylphenyl pyruvamide was synthesized following a similar procedure used to make the other pyruvamides (**9a,b**) with the exception of requiring slightly longer reaction times.

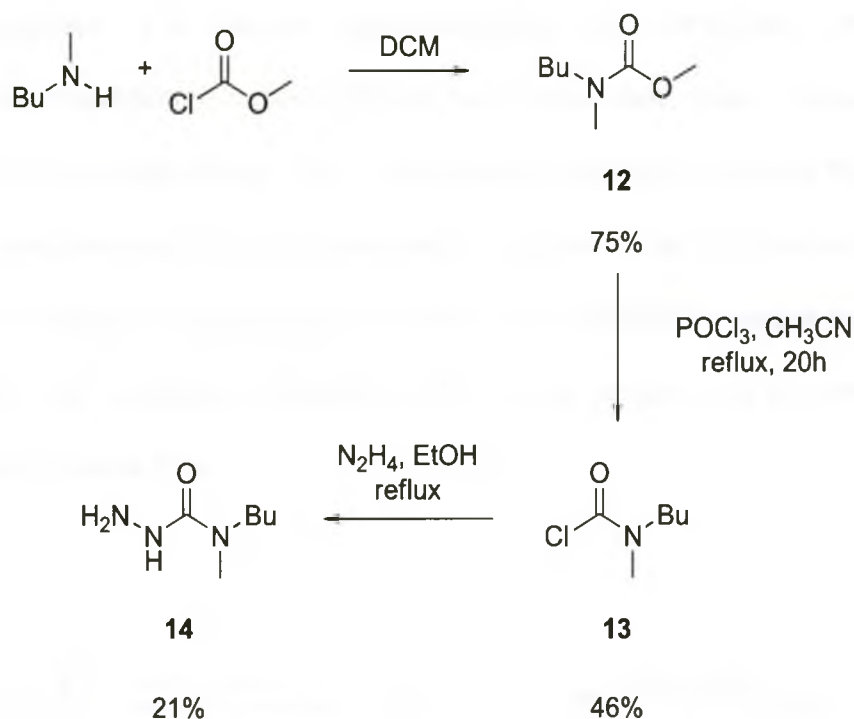


Scheme 3.1 - Synthetic route of *N*-Methylphenyl pyruvamide.

Pyruvoyl chloride would again be created *in situ* and added to *N*-methylaniline. Compound **11** was purified via column chromatography with dichloromethane in 48% yield.

The *N*-methylated semicarbazide would prove to be more difficult to synthesize. Initial attempts followed the same routes as that for the 4-semicarbazides discussed earlier in chapter two (Scheme 2.1) with no success. An alternative approach was employed (Scheme 3.2).

Methyl chloroformate was coupled with *N*-methyl-*n*-butylamine producing the resulting carbamate **12** in 75% yield without the need for further purification. The synthesis of 4-semicarbazides in Chapter 2 resulted from a carbamate reacting with hydrazine under reflux conditions. However, the likely mode of formation is through the creation of an isocyanate *in situ* that reacts with hydrazine. Compound **12** cannot undergo such a transformation and as such was converted to the more reactive species **13**.

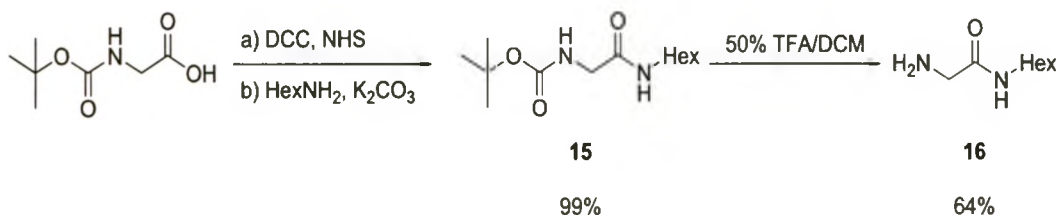


Scheme 3.2 - Synthetic route of 4,4-Butylmethylsemicarbazide.

Analagous *N,N*-dialkylcarbamoyl chlorides were synthesized by Hoshino and co-workers.⁸³ In this case, the reaction time was longer than those reported for similar compounds. The carbamate starting material would still be observed when the reaction was halted prior to twenty hours. Compound **13** would be produced in 46% after reaction of **12** with 5 equivalents of phosphorous oxychloride. Care was required during the quenching of the excess phosphorous oxychloride as when performed too quickly yields were significantly reduced.

4,4-Butylmethylsemicarbazide was synthesized in 21% yield when **13** was added to hydrazine. Attempts in acetonitrile resulted in considerably lower yields.

The synthesis of a 2-amino-*N*-hexylacetamide was carried out from the initial coupling of *N*-(*tert*-butoxycarbonyl)glycine with hexylamine. Initial attempts employed *N,N'*-dicyclohexylcarbodiimide with 1-hydroxybenzotriazole as would be expected in traditional peptide coupling resulted in moderate to low yields. Purification was difficult due to the presence of dicyclohexylurea (DCC). An alternative approach created a stable active ester, the complete precipitation of the urea species and required no further purification (Scheme 3.3).

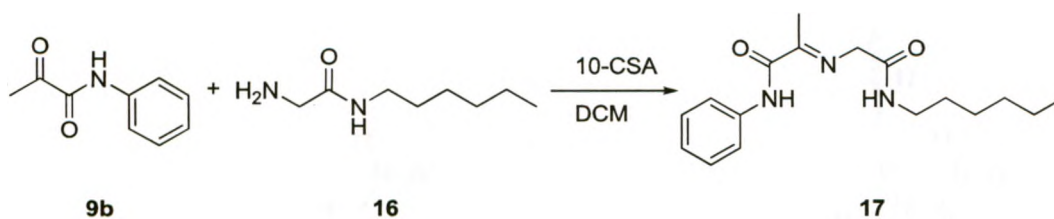


Scheme 3.3 - Synthetic route to 2-amino-*N*-hexylacetamide.

The use of *N*-hydroxysuccinimide in the creation of an active ester intermediate was essential in increasing yields (quantitative) and purity of the final product, **15**. Deprotection of **15** was carried out overnight resulting in **16** with 64% yield and not requiring further purification. Initial attempts at the de-protection resulted in lower yields as the length of time, 18 hours, is longer than might be anticipated for this process.

Initial attempts at the condensation between 2-amino-*N*-hexylacetamide and *N*-phenylpyruvamide were unsuccessful. Traditional approaches using a Dean-Stark

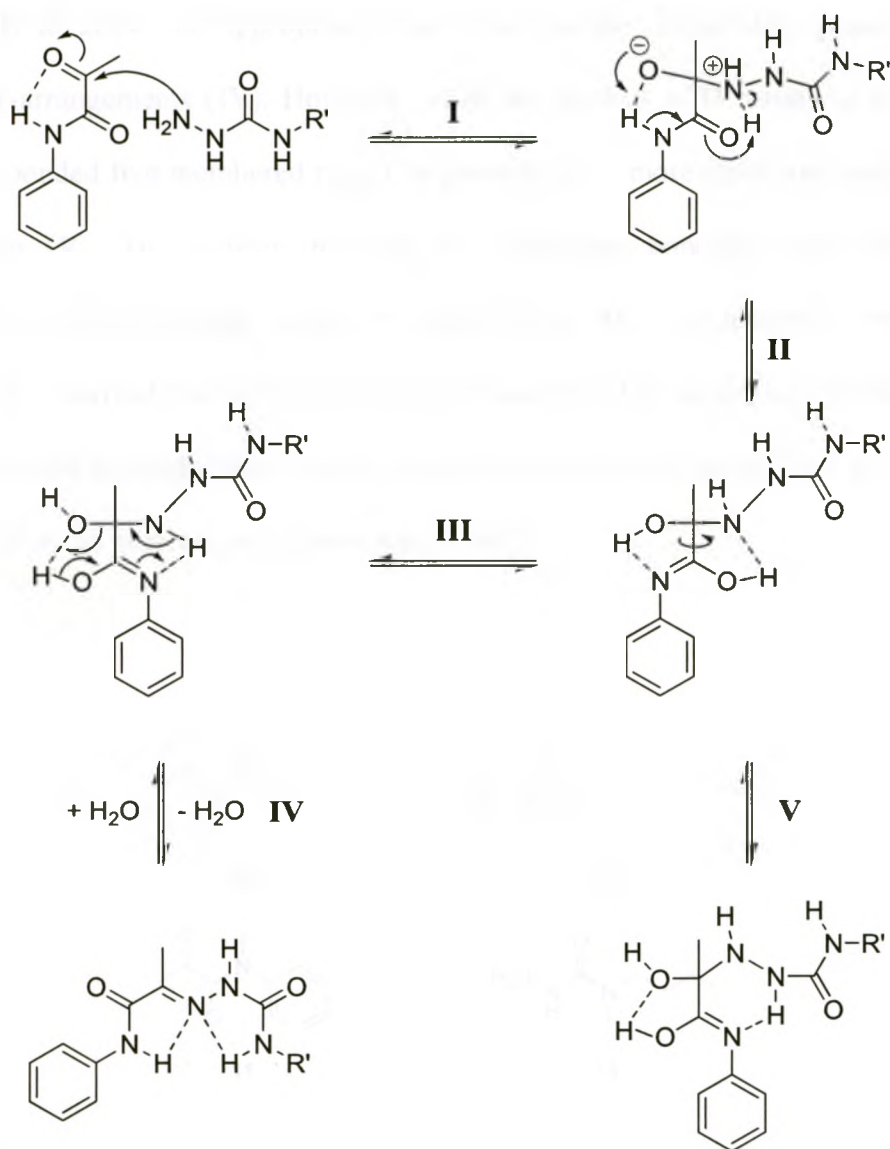
apparatus, refluxing in methanol, ethanol, and molecular sieves in dichloromethane or acetonitrile resulted in no formation of the condensed product. The use of anhydrous 10-camphorsulfonic acid was crucial (Scheme 3.4).



Scheme 3.4 - Route to Schiff base receptor.

Compound 17 was successfully synthesized; however purification was very difficult. Attempts at purification resulted in the receptor breaking apart to the starting materials or streaking during chromatographic separation. As a result of the inability to purify this receptor, no titration data were collected.

3.2.2 Kinetics – removal of hydrogen bond donors.



Scheme 3.5 - Possible condensation mechanism of semicarbazone formation.

The mechanism described by Young and co-workers of Schiff base formation from pyruvamide can be expanded upon and applied to semicarbazone formation (Scheme 3.5). The carbonyl carbon is stabilized to initial nucleophilic attack (**I** and **II**)

through internal hydrogen bonding. A rotation in the carbinolamine structure is likely to occur (III) to allow the appropriate orientation for the dehydration process through internal re-arrangements (IV). However, while the product of II results in an internally hydrogen bonded five membered ring, it is possible for a more stable six membered ring to develop (V). To confirm the role that hydrogen bonding plays between the intermediates and chloride anion in accelerating the condensation process, we sequentially removed the sites for hydrogen bonding. The following combinations of methylated and un-methylated starting reagents were tested (Figure 3.5): **11** + **8a**, **11** + **14**, **9b** + **14** in the presence and absence of TBACl.

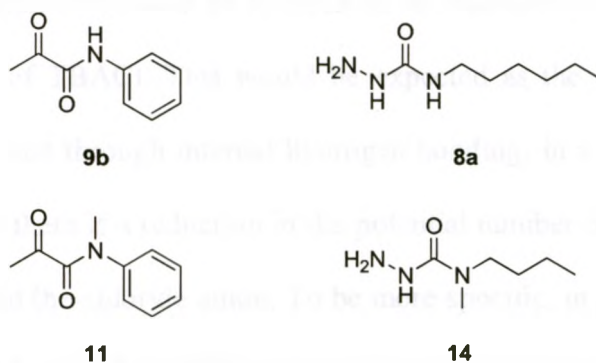


Figure 3.5 - Methylated and unmethylated components towards semicarbazone formation.

Case: 11 + 8a

In the first case, **11 + 8a**, there was no change in the spectra in the presence or absence of TBACl. These reactions were monitored for 4 days with no changes observed. As would be expected from the proposed mechanisms for Schiff base formation as reported by Young and co-workers, internal hydrogen bonding through the amide of compound **9b** would be important in increasing the electrophilicity of the carbonyl. In the absence of this internal hydrogen bond (**9b + 8a**), there is no reaction observed.

Case: 11 + 14

The combination of **11** and **14** resulted in no reaction even after 4 days in the absence or presence of TBACl. This would be expected as the electrophilicity of the carbonyl is not increased through internal hydrogen bonding, in a similar manner to the case of **11 + 8a**. Also there is a reduction in the potential number of interactions with the semicarbazide unit and the chloride anion. To be more specific, in the case of **8a** there is a urea motif which is known for binding anions. However in the case of **14**, this motif is not present with substitution of hydrogen for a methyl group.

Case: 9b + 14

In the absence of TBACl there were no changes observed. However, in the presence of one equivalent of TBACl a reaction takes place, though only occurring very slowly (Figure 3.7).

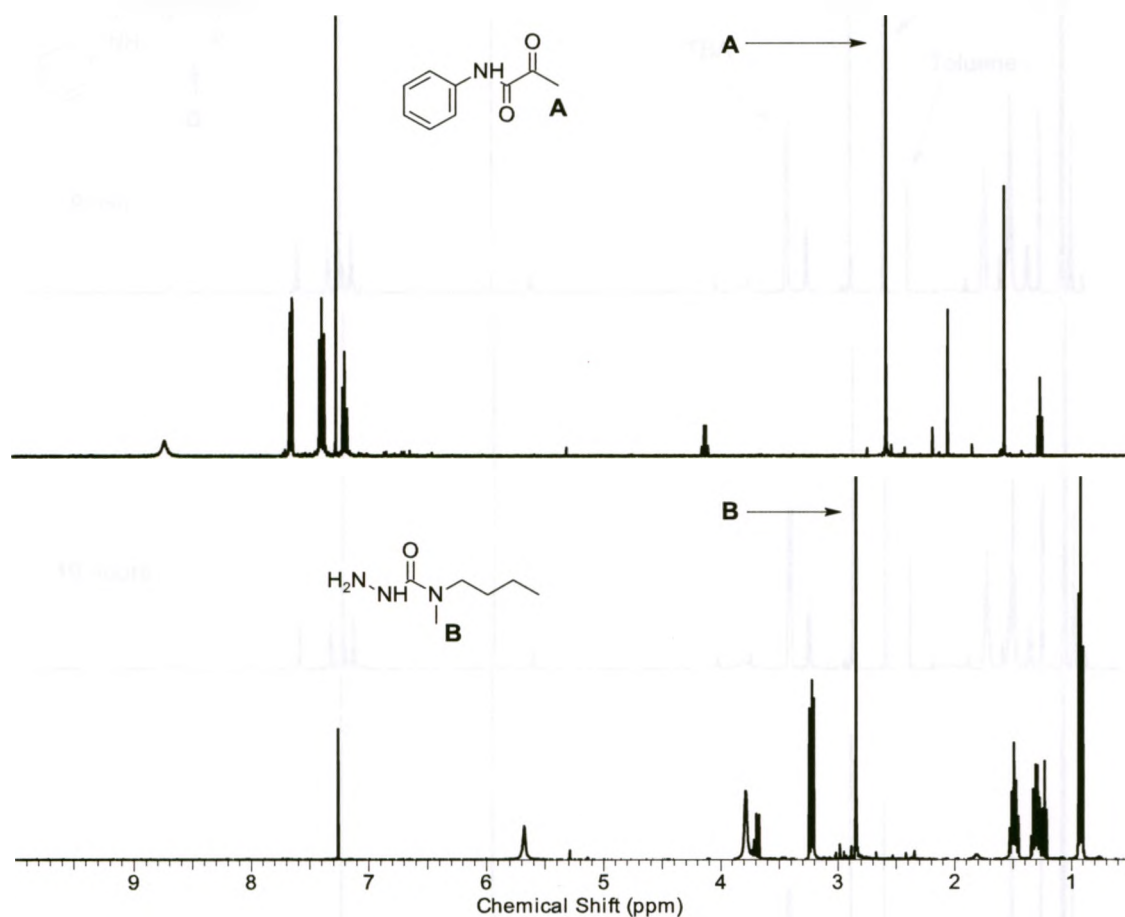


Figure 3.6 - ^1H Spectra of phenylpyruvamide, **9b** and 4,4-butylmethylsemicarbazide, **14** in CDCl_3 at 298K.

The decrease in starting material was gradual. Though the spectra of the desired condensed product is not known the methyl group near the newly formed imine is usually in the range of 2 ppm to 2.3 ppm (C, Figure 3.7). The initial rate was determined to be $6.0 \times 10^{-7} \text{ M min}^{-1}$ based upon the predicted product methyl resonances. The shifts in amide peaks of starting material or possible products are a result of hydrogen bonding with chloride.

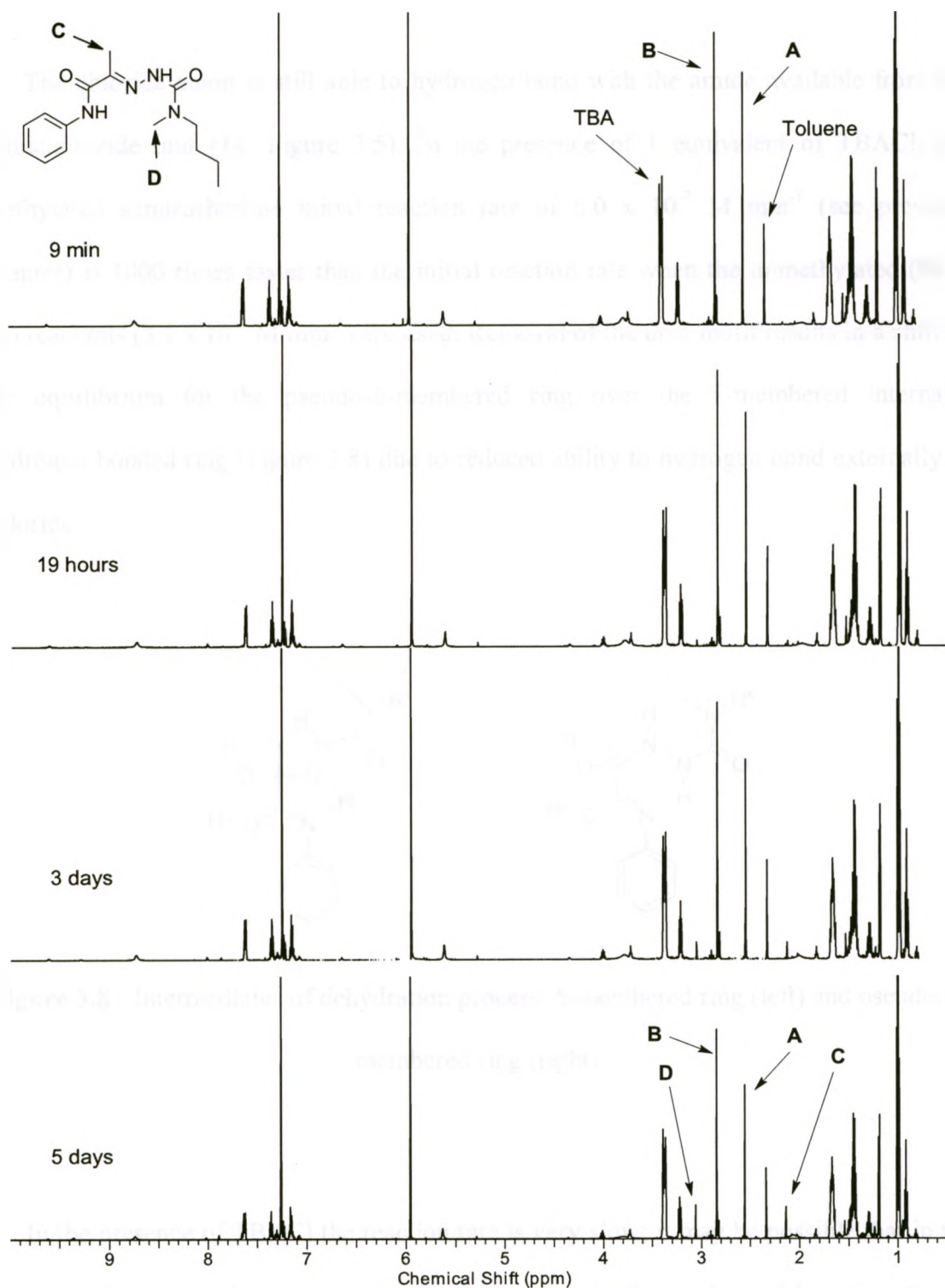


Figure 3.7 - Acceleration of semicarbazone condensation (**9b** + **14**) in the presence of TBACl.

The chloride anion is still able to hydrogen bond with the amide available from the semicarbazide unit (**14**, Figure 3.5). In the presence of 1 equivalent of TBACl, the methylated semicarbazone initial reaction rate of $6.0 \times 10^{-7} \text{ M min}^{-1}$ (see previous chapter) is 1000 times faster than the initial reaction rate when the unmethylated (**9b** + **8a**) reactants ($3.1 \times 10^{-4} \text{ M min}^{-1}$) are used. Removal of the urea motif results in a shift of the equilibrium for the pseudo-6-membered ring over the 5-membered internally hydrogen bonded ring (Figure 3.8) due to reduced ability to hydrogen bond externally to chloride.

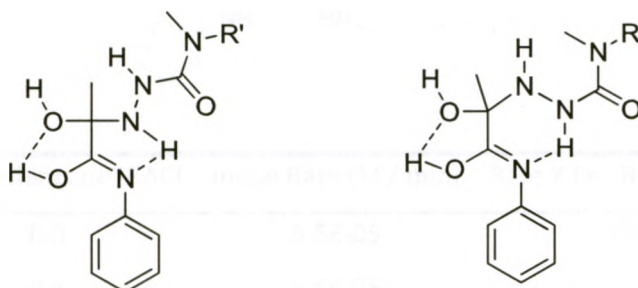


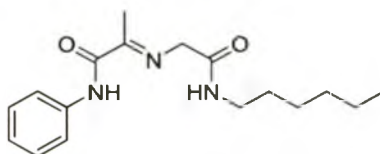
Figure 3.8 - Intermediates of dehydration process: 5-membered ring (left) and pseudo-6-membered ring (right).

In the presence of TBACl the reaction rate is very slow; it may be possible that in the absence of chloride, the reaction rate is much slower and not observable within 4 or 5 days.

3.2.3 Kinetics of Schiff base formation in the presence of TBACl

The use of a 2-aminoacetamide should act in a twofold manner: i) with the urea motif removed, will there be any increase in condensed product formation in the presence of TBACl? and ii) whether TBACl acceleration applies to primary amines as well. The Schiff base formation was tested with a primary amine containing analogous hydrogen bonding sites (compound **16**, 2-amino-*N*-hexylacetamide) and phenylpyruvamide (**9b**). Acceleration in Schiff base formation was observed.

Table 5 - Increase in initial rates of formation for receptor **17** in the presence of various TBACl equivalents.



X Equivalents of TBACl	Initial Rate (M / min)	Rate X Eq./Rate 0 Eq.
0.0	5.5E-05	1.00
0.1	5.5E-05	1.00
0.2	5.6E-05	1.02
0.4	6.0E-05	1.09
0.5	5.9E-05	1.07
0.6	6.2E-05	1.12
0.8	6.7E-05	1.22
1.0	9.2E-05	1.67
2.0	1.1E-04	2.11
3.0	1.1E-04	2.06

The acceleration was nominal compared to the uncatalyzed reaction (Table 5) and not as great as observed with the semicarbazides (Table 4). This slight effect with the presence of chloride may be weak hydrogen bonding with an intermediate in the reaction. The association of TBACl with 2-amino-*N*-hexylacetamide was observed to be approximately zero during a titration study of the two species as there were insignificant changes of chemical shift ($\Delta\delta < 0.01$ ppm) of the amine/amide. This suggests that the anion must interact with an intermediate species of the reaction rather than bringing the components together.

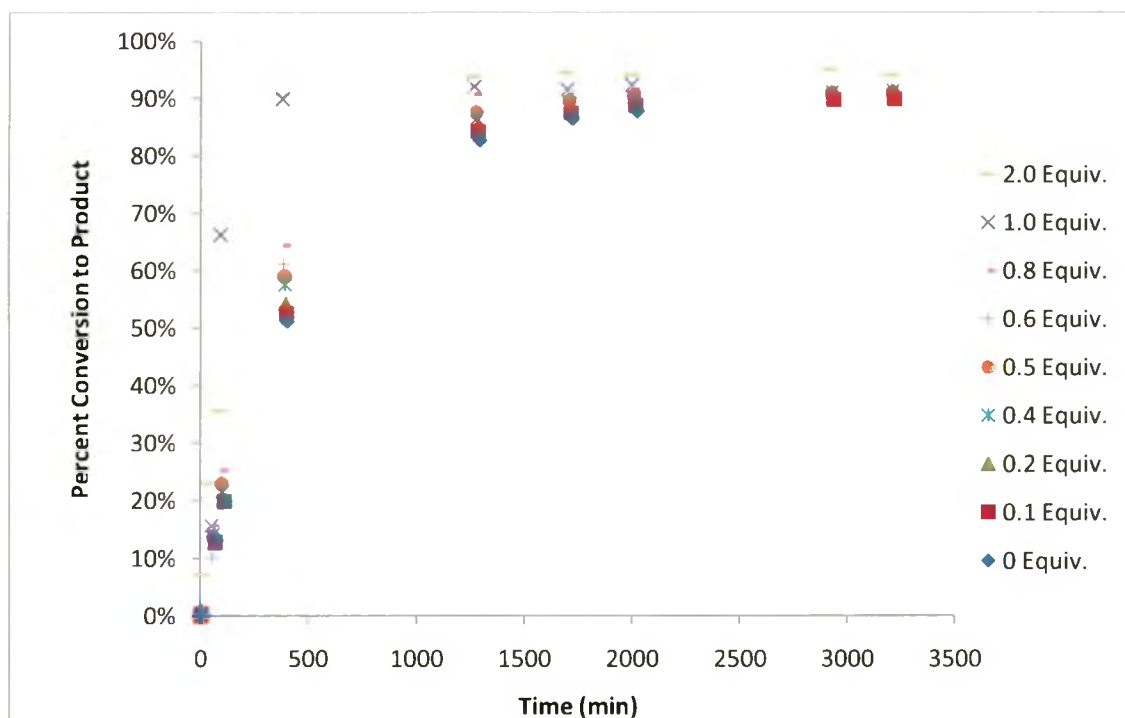


Figure 3.9 - Percent conversion from phenylpyruvamide to condensed receptor **17**.

The fact that there is a reduction in the number of hydrogen bonding sites would reduce the interaction with the chloride anion present. Recalling from the previous chapter, the reaction of 4-hexylsemicarbazide and phenylpyruvamide in the presence of 1.0 equivalents of TBACl reached 80% within approximately 60 minutes, where as when 2-amino-*N*-hexylacetamide is used, approximately 80% completion occurs within 400 minutes. A plot of the natural logs of initial rates versus concentration of chloride can be made to determine the order for chloride.

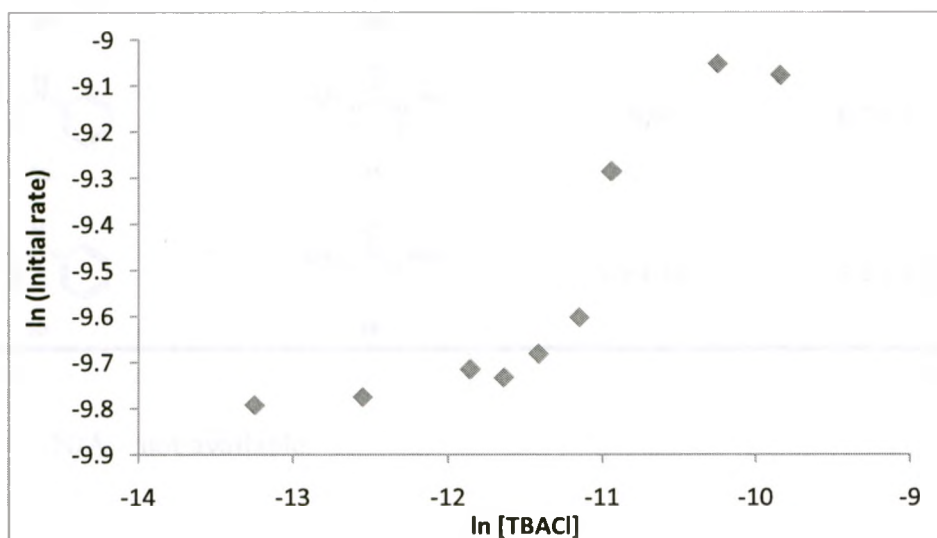
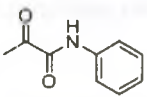
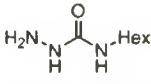
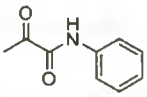
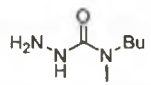
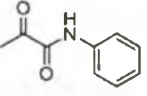
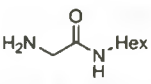


Figure 3.10 - Plot of natural logs of initial rates versus concentration of TBACl for Schiff base receptor 17.

In this case, the plot does not produce a linear distribution (Figure 3.10). This would suggest that there is a very low order of reaction with respect to chloride. As

observed in Table 6 there is very little acceleration in the reaction rates as compared to the control confirming the lack of a linear correlation. Therefore chloride does not accelerate Schiff base formation.

Table 6 – Summary of initial rates of reaction

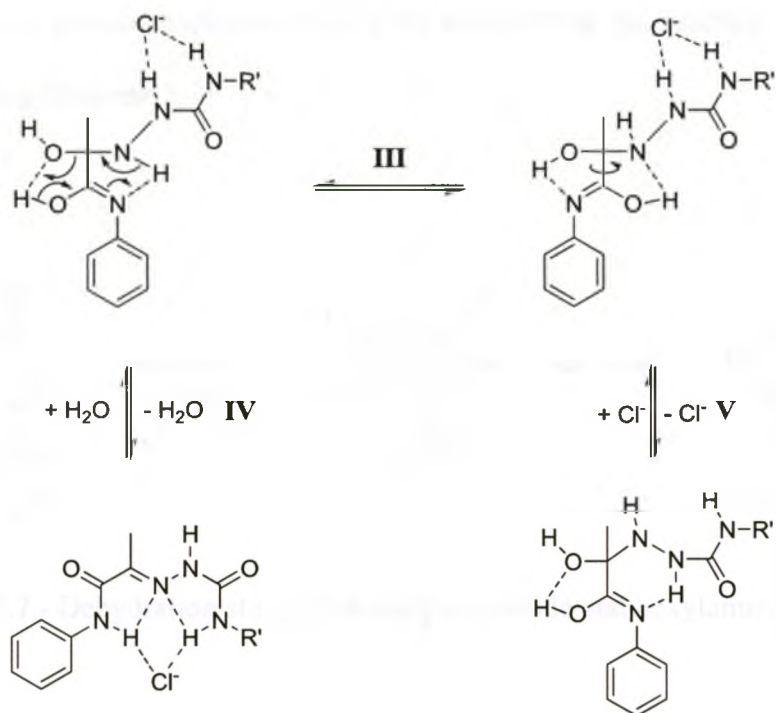
Initial Rate of Reaction (M min^{-1})		0 Eq TBACl	1.0 Eq TBACl	
	+		1.3×10^{-6}	3.1×10^{-4}
9b		8a		
	+		N/A	6.0×10^{-7}
9b		14		
	+		5.5×10^{-5}	9.2×10^{-5}
9b		16		

- N/A – not available.

However, it is interesting to note that when comparing the uncatalyzed/untemplated conditions between the condensations of the primary amine and that of the semicarbazide, the primary amine displays a higher initial rate of reaction of $5.5 \times 10^{-5} \text{ M min}^{-1}$ compared to $1.3 \times 10^{-6} \text{ M min}^{-1}$ of the semicarbazide. Unfortunately, there are very few literature comparisons of nucleophilic attack of an amine or semicarbazide upon a carbonyl compound. One such report contains the nucleophilic attack of a semicarbazide

and glycine on pyridine-4-carboxaldehyde. The semicarbazide has a reaction rate approximately 100 times faster than that of glycine.⁸⁴ It would be expected for the semicarbazide to attain a higher rate of reaction compared to acetamide as observed by Sander *et al.* However, in our case the internal hydrogen bonding (6-membered ring) of the semicarbazide (which is more stable) retards the reaction rate preventing the required internal proton shifts for dehydration. The primary amine which lacks the ability to adopt an internally hydrogen bonded pseudo-6-membered ring to retard the reaction, results in a high reaction rate.

Though the primary amine attains a higher reaction rate compared to the semicarbazide, the reverse occurs in the presence of chloride. The semicarbazide has a higher initial rate of reaction ($3.1 \times 10^{-4} \text{ M min}^{-1}$) in the presence of one equivalent of TBACl, while it is $9.2 \times 10^{-5} \text{ M min}^{-1}$ for the primary amine. In the presence of chloride, it is likely the 5-membered ring is favoured in the equilibrium process due to the urea motif hydrogen bonding externally to chloride rather than internally (Scheme 3.6).

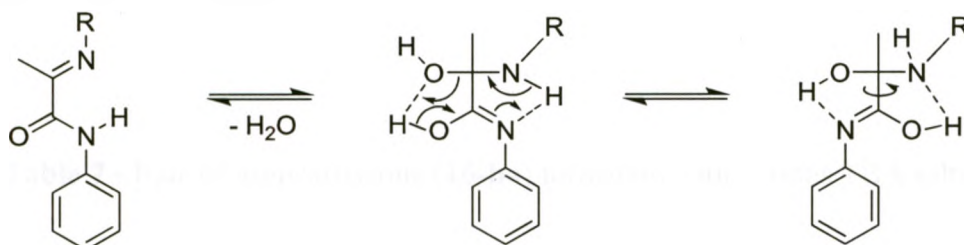


Scheme 3.6 – Equilibrium between 5-membered ring (top left) and pseudo-6-membered (bottom right) internal hydrogen bonding rings.

The presence of chloride disrupts this internal bonding shifting the equilibrium towards the desired 5-membered ring. The proton shifts required to the release of water is possible in this conformation. As the amount of chloride present increases, the equilibrium likely shifts increasingly to the 5-membered ring allowing for increases in product formation and reaction rate.

A preliminary study was performed to qualitatively observe the reaction between phenylpyruvamide and hexylamine in the absence of TBACl. The reaction was complete within 2 days with a high level of conversion (approx. 90%). The semicarbazone does not achieve full conversion in that amount of time. Hexylamine does not present the

possibility of a pseudo-6-membered ring to arise during the reaction, but only the 5-membered ring (Scheme 3.7).



Scheme 3.7 - Dehydration steps of phenylpyruvamide and hexylamine (R = Hexyl).

This helps to further confirm the possibility of internal hydrogen bonding from the semicarbazide unit in retarding the condensation reaction.

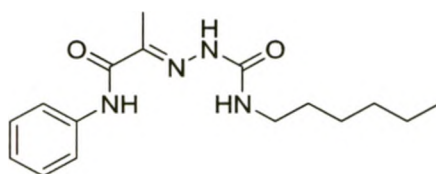
Another qualitative test was performed to examine whether the presence of TBACl would accelerate any Schiff base formation. Acetophenone and hexylamine were monitored in the presence and absence of TBACl. In both cases, no reaction was observed showing that the carbinolamine transition states alone are not stabilized in the presence of TBACl. This result confirms the necessity for additional hydrogen bonding sites to associate internally aiding in proton transfer cascades.

3.2.4 Kinetics of semicarbazone formation with various anions

To further investigate hydrogen bonding of the urea motif in the mechanism of semicarbazone formation, various tetrabutylammonium salts (hydrogen sulfate, *p*-toluene

sulfate, chloride, bromide, iodide, perchlorate, hexafluorophosphate, and acetate) were used in the reaction. It would be expected that good hydrogen bond acceptors would result in a increased rate of reaction as the equilibrium would be shifted to the 5-membered internally hydrogen bonded ring.

Table 7 - Rate of semicarbazone (**10-ba**) formation with various TBA salts.



TBA Salt (X)	Initial Rate (M / min)	Rate TBA X / Rate control	pKa of HX ⁸⁵
HSO ₄ ⁻	2.3E-02	17224	-3.0, 1.99*
OTs	2.1E-02	15896	-1.0
Cl ⁻	3.1E-04	234	- 7.0
Br ⁻	3.7E-05	28	- 9.0
I ⁻	2.3E-05	17	- 10.0
ClO ₄ ⁻	1.5E-05	11	- 10.0
PF ₆ ⁻	1.1E-05	8	-
AcO ⁻	7.2E-06	5	4.76
Control	1.3E-06	1	N.A.

- *The pKa of -3.0 is for H₂SO₄, the pKa of HSO₄⁻ is 1.99. (-) – there is no pKa data available. N.A. – not applicable.

Table 7 summarizes the initial rate of formation of compound **10-ba**. As would be expected the highest acceleration is in the presence of the acid hydrogensulfate. Acetate

appears to have the slowest initial rate (Figure 3.11), however this rate appears to be constant as full conversion is observed within 3 days (Figure 3.12). The hydrogen bond acceptor strength of halide anions decreases with increasing size. This parallels the decrease in the initial rates of reaction observed. Full conversion is achieved with good and moderate hydrogen bond acceptors.

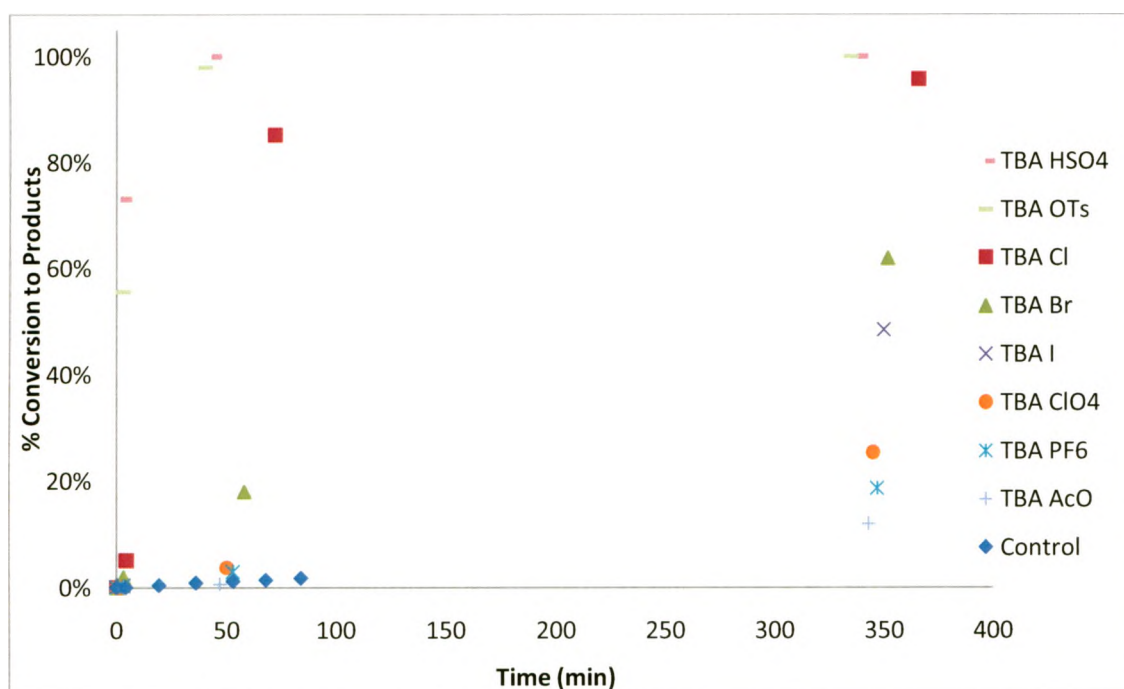


Figure 3.11 – Initial percent semicarbazone conversion from phenylpyruvamide in the presence of 1 eq. of TBAX.

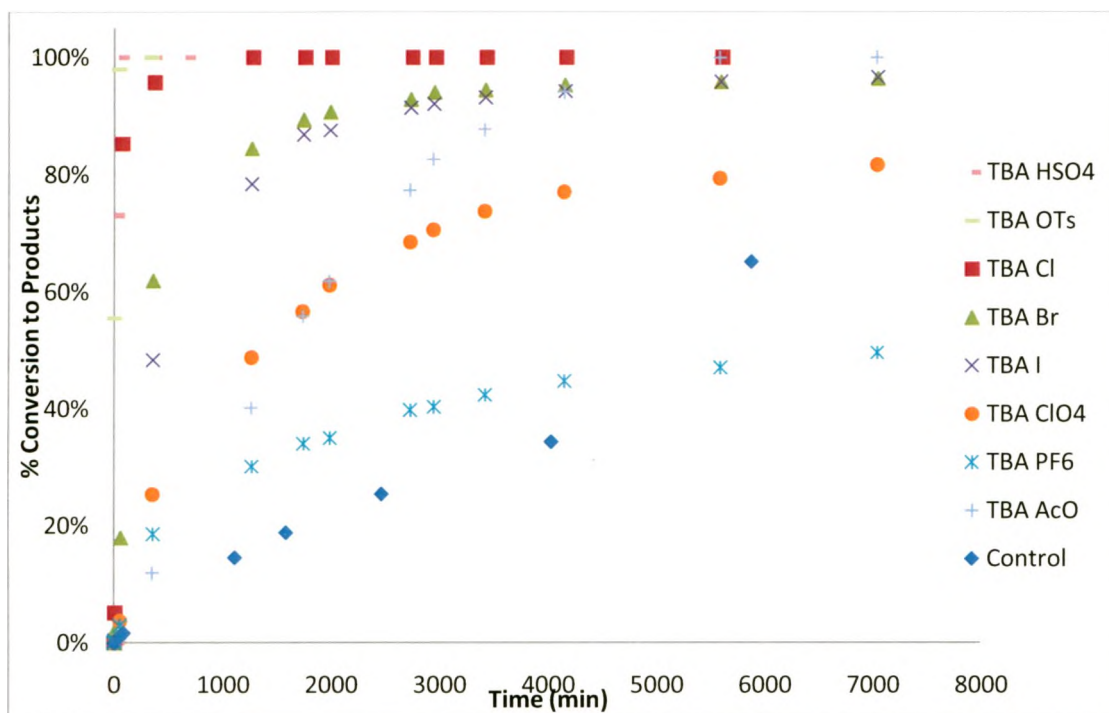


Figure 3.12 - Overall percent conversion of semicarbazone from phenylpyruvamide in the presence of 1 eq. of TBAX.

Perchlorate and hexafluorophosphate which are known to be poor hydrogen bond acceptors resulted in lower reaction rates. In both of these cases, there is not full conversion to the product semicarbazone. Perchlorate plateaus conversion to approximately eighty percent while that of hexafluorophosphate is fifty percent.

In the case of acetate and hydrogen sulfate, these anions can be acting as a base or an acid respectively. These anions would not only behave as hydrogen bond acceptors and thus stand outside of the correlations observed.

The uncatalyzed reaction (control), in the absence of any anion does not reach full conversion in the time monitored. After approximately 5 days, monitoring was stopped

due to changes in the volumes of the reaction vessels. These changes result in concentration variations that would influence the reaction rates and as such, the data near these end points can only be used as a qualitative view of the reaction progress.

The tetrabutylammonium (TBA) cation does not appear to influence the rate. If TBA does affect the rate, then when anions of similar hydrogen bond acceptor strength are used, there should be no change in reaction rates. Bromide and iodide are moderate hydrogen bond acceptors and a change in the reaction rate is still observed albeit relatively small. Further testing with various cationic sources would provide more insight into this area.

The initial rates of reaction show a correlation with increasing hydrogen bonding acceptor strength of the anion present. The increases in basicity of the anions results in an increase in the hydrogen bonding acceptor strength. When a strong hydrogen bond acceptor is used, the association between the anion and urea motif increases. The equilibrium is shifted further to the 5-membered internal ring away from the pseudo-6-membered ring (Scheme 3.6). The 5-membered ring allows for a proton shift leading to dehydration. Whereas if a poor hydrogen bond acceptor is present, then the equilibrium lies towards the internally hydrogen bonded pseudo-6-membered ring.

3.2.5 Summary and Conclusions

Semicarbazone receptors **10-aa** and **10-ba** displayed preferential binding for chloride over other anions albeit lower compared to pyridine dicarboxamide. As there are three hydrogen bond donor sites, there are at least two binding conformations possible:

urea-like and pyridine dicarboxamide-like. It cannot be determined as to what conformation the receptors adopt upon anion recognition.

Chloride was observed to accelerate the formation of **10-ba** and **10-aa**. Through the sequential removal of hydrogen bonding sites it was determined that the chloride anion likely aids in the equilibrium among two possible transition state conformations. The use of a semicarbazide which contains a urea motif, can internally hydrogen bond to form a pseudo-6-membered ring. In the dehydration process there is an isoamide 5-membered ring that forms allowing for a concerted proton shift to occur leading to water loss. The desired amide is also returned in this process. However, the possibility of the pseudo-6-membered ring prevents this rearrangement to occur and results in a retardation of the reaction.

The presence of chloride and other hydrogen bond acceptors bind the urea motif present shifting the equilibrium from the pseudo-6-membered ring to the 5-membered ring resulting in product formation. The hydrogen bond acceptor strength of the anions influences the reaction rate. The stronger acceptors result in increased rates of reaction as the equilibrium is further shifted to the 5-membered ring.

The acceleration process is not observed in the case of a primary amine, 2-amine-*N*-hexylacetamide, as there is no possibility for an internal pseudo-6-membered ring to form and retard the reaction rate. In the general case of Schiff base formation, acetophenone and hexylamine, no reaction or acceleration was observed. Anion acceleration is only observed within the semicarbazide and pyruvamide system present

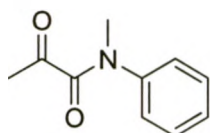
here. The elaborate nature of design and hydrogen bonding has been displayed in our system presented.

3.3. Experimental

General Considerations

Please see previous chapter.

N-Methylphenyl pyruvamide (11)



To a 100 mL round bottomed flask containing one drop of dimethylformamide, 25 mL of DCM and 1.8 mL (20.6 mmol) of oxalyl chloride was 1.65 mL (23.7 mmole) of pyruvic acid added in 25 mL of DCM slowly at room temperature. Upon completion of addition, the solution was left to stir for three hours. This solution was then added dropwise to a second 250 mL RBF containing 2.1954 g (26.1 mmol) sodium bicarbonate and 2.6 mL (24.0 mmole) of *N*-Methylaniline in 50 mL DCM. After four hours, water (75 mL) was added and the organics extracted with DCM (3 x 50 mL). The combined organics were washed with water (1 x 100 mL), 5% HCl (1 x 75 mL), dried with

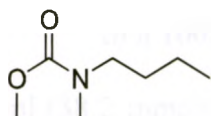
magnesium sulfate, filtered and the volatiles evaporated. The product was isolated chromatographically (DCM) yielding a clear yellow oil 2.016 g (48%).

^1H NMR (CDCl_3 , δ): 7.35 (m, 3 H), 7.16 (d, $J = 7.0$ Hz, 2 H), 3.32 (s, 3 H), 2.19, (s, 3 H).

^{13}C NMR (CDCl_3 , δ): 197.7, 167.1, 141.4, 129.6, 128.12, 126.27, 36.3, 27.6.

HRMS: calc for $\text{C}_{10}\text{H}_{11}\text{NO}_2$: 177.0790, found: 177.0795

***N,N*-Butylmethylcarbamate (12)**



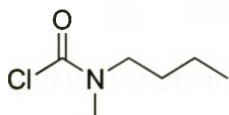
In a 100 ml RBF, 5 mL (42.2 mmole) of *N*-Methylbutylamine is stirred with 3.645 g (43.4 mmole) of sodium bicarbonate with 50 mL dichloromethane in an ice bath. To this solution, 3.5 mL (45.5 mmole) of methyl chloroformate in 10 mL DCM was added dropwise. This solution was allowed to stir at room temperature for six hours before water (60 mL) was added. The organics were then extracted with DCM (3 x 50 mL) and combined before washing with 1% HCl (75 mL), water (100 mL), dried with magnesium sulfate, filtered and the volatiles removed yielding a clear liquid 7.079 g (75%) requiring no further purification.

^1H NMR (CDCl_3 , δ): 3.64 (s, 3 H), 3.19 (m, 2 H), 2.86 (d, $J = 12.9$ Hz, 3 H), 1.46 (m, 2 H), 1.26 (m, 2 H), 0.89 (t, $J = 7.4$ Hz, 3 H).

^{13}C NMR (CDCl_3 , δ): 156.9, 52.3, 48.4, 48.3, 34.4, 33.7, 29.9, 29.5, 19.7, 13.7.

HRMS: calc for $\text{C}_7\text{H}_{15}\text{NO}_2$: 145.1103, found: 145.1190

***N,N*-Butylmethylcarbonyl chloride (13)**

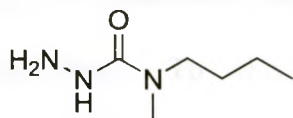


In a 100 mL RBF 1.015 g (7.0 mmole) of Methyl *N,N*-butylmethylcarbamate, 3.5 ml (38.2 mmole) of phosphorous oxychloride in 50 mL acetonitrile was refluxed for 20 hours. The reaction vessel was then cooled to room temperature before slowly being poured on ice. The organics were then extracted with DCM (4 x 60 mL). The combined organics were washed with 1M sodium bicarbonate (2 x 100 mL), water (2 x 100 mL), dried with magnesium sulfate and finally removal of the volatiles. The resulting 0.0460 g (46%) of clear green liquid product required no further purification.

^1H NMR (CDCl_3 , δ): 3.37 (dt, $J = 24.6$ Hz, 7.4 Hz, 2 H), 3.11(s, 1.5 H), 3.02 (s, 1.5 H), 1.53 (m, 2 H), 1.29 (m, 2 H), 0.89 (q, $J = 7.4$ Hz, 3 H).

^{13}C NMR (CDCl_3 , δ): 148.9, 52.6, 36.5, 29.0, 19.5, 13.5.

HRMS: calc for $\text{C}_6\text{H}_{12}\text{ClNO}$: 149.0607, found: 149.0607

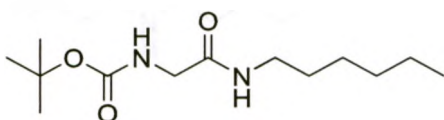
4,4-Butylmethylsemicarbazide (14)

In a 100 mL RBF, 4 mL (49.3 mmol) of hydrazine and 2.548 g (30.3 mmole) of sodium bicarbonate in 20 mL ethanol were stirred in an ice bath. To this solution 4.41 g (29.5 mmole) of *N,N*-Butylmethylcarbamyl chloride in 20 mL ethanol was slowly added. The reaction was stirred for three hours after which time the organics were extracted with DCM (3 x 50 mL). The combined organics were then washed with water (100 mL), dried and the volatiles evaporated. Flash column chromatography (8:2 Ethylacetate:DCM) yielded a clear yellow oil, 0.915 g (21%).

^1H NMR (CDCl_3 , δ): 5.88 (s, 1 H), 3.79 (s, 2 H), 3.22 (t, $J = 7.4$ Hz, 2 H), 2.85 (s, 3 H), 1.49 (m, 2 H), 1.29 (m, 2 H), 0.92 (t, $J = 7.4$ Hz, 3 H).

^{13}C NMR (CDCl_3 , δ): 160.2, 48.6, 33.8, 30.0, 19.9, 13.8.

HRMS: calc for $\text{C}_6\text{H}_{15}\text{N}_3\text{O}$: 145.1215, found: 145.1216

***tert*-Butyl-*N*-[(hexylcarbamoyl)methyl]carbamate (15)**

In a 250 mL RBF 3.107 g (17.7 mmole) of *N*-(*tert*-Butoxycarbonyl)glycine, 2.061 g (17.9 mmole) of *N*-hydroxysuccinimide in 150 mL of tetrahydrofuran were stirred in an ice bath. To this solution was added 3.652 g (17.7 mmole) of *N,N'*-Dicycloheptylcarbodiimide slowly. The reaction was stirred for 18 hours and then stored at -30 °C for 6 hours. Any precipitate was filtered off with the filtrate being added dropwise to a second 500 mL RBF containing 2.35 mL (17.7 mmol) of hexylamine, 2.498 g (18.1 mmol) of potassium carbonate and 250 mL tetrahydrofuran. The reaction was left to stir for 18 hours. The organics were then extracted with DCM (3 x 80 mL). The combined organics were washed with 5% HCl (100 mL), water (2 x 150 mL), dried and the volatiles removed yielding a white liquid 4.546 g (99%).

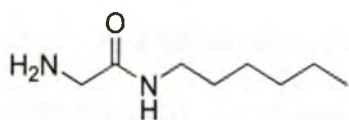
^1H NMR (CDCl_3 , δ): 6.14 (s, 1 H), 5.17 (s, 1 H), 3.75 (d, $J = 5.5$ Hz, 2 H), 3.26 (dt, $J = 6.3$ Hz, 7.0 Hz, 2 H), 1.49 (m, 2 H), 1.45 (s, 9 H), 1.28 (m, 6 H), 0.87 (t, $J = 7.0$ Hz, 3 H).

^{13}C NMR (CDCl_3 , δ): 169.4, 156.1, 79.9, 44.2, 39.4, 31.4, 29.4, 28.2, 26.4, 22.4, 13.9.

EI LRMS m/z (Intensity): 258 (8, M^+), 202 (41), 185 (39), 128 (30), 75 (36).

HRMS: calc for $\text{C}_{13}\text{H}_{26}\text{N}_2\text{O}_3$: 258.1943, found: 258.1946.

2-amino-*N*-hexylacetamide (16)



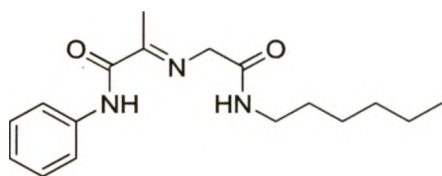
In a 50 mL RBF 3.73 g (14.4 mmol) of **15** is stirred in 4 mL of DCM on ice. To this solution 6 mL of trifluoroacetic acid is added slowly and the reaction left to stir for 18 hours. The reaction vessel is then poured on ice and cooled in an ice bath while being basified to a pH of 9 with 1 M sodium hydroxide. The organics were then extracted with ethylacetate (4 x 30 mL) and combined before washing with water (2 x 80 mL) and drying. The volatiles were then removed yielding a light green white solid 1.47 g (64%) that required no further purification.

$^1\text{H NMR}$ (CDCl_3 , δ): 7.24 (s, 1 H), 3.34 (s, 2 H), 3.27 (q, $J = 7.0$ Hz, 2 H), 1.51 (m, 4 H), 1.29 (m, 6 H), 0.88 (t, $J = 7.0$ Hz, 3 H).

$^{13}\text{C NMR}$ (CDCl_3 , δ): 172.4, 44.5, 38.8, 31.3, 29.4, 26.4, 22.3, 13.8.

HRMS: calc for $\text{C}_8\text{H}_{18}\text{N}_2\text{O}$: 158.1419, found: 158.1415

Compound 17



In a 50 mL RBF flask, 0.088 g (0.538 mmol) of phenyl pyruvamide (**9b**), 0.083 g (0.524 mmol) of 2-amine-*N*-hexylacetamide (**20**) and 0.024 g (0.104 mmol) of 10-camphosulfonic acid were stirred in DCM for 24 hours. Sodium sulfate was then added and filtered. The volatiles of the filtrate were removed yielding 0.146 g of a crude oil.

^1H NMR (CDCl_3 , δ): 9.18 (s, 1 H), 7.58 (d, $J = 7.8$ Hz, 2 H), 7.32 (t, $J = 7.4$ Hz, 2 H), 7.12 (t, $J = 7.4$ Hz, 1 H), 7.06 (t, $J = 5.9$ Hz, 1 H), 4.06 (s, 3 H), 3.32 (q, $J = 7.0$ Hz, 2 H), 2.14 (s, 3 H), 1.26 (m, 6 H), 0.86 (m, 3 H).

^{13}C NMR (CDCl_3 , δ): 168.7, 165.6, 161.1, 136.9, 128.9, 124.5, 119.7, 55.31, 39.2, 31.3, 29.5, 26.5, 22.5, 13.9, 13.6.

HRMS: calc for $\text{C}_{17}\text{H}_{25}\text{N}_3\text{O}_2$: 303.1947, found: 303.1945

Bibliography

- ¹ Dutzler, R.; Campbell, E.B.; Cadene, M.; Chait, B.T.; Mackinnon, R. *Nature* **2002**, *415*, 287-294.
- ² Gale, P.A. *Acc. Chem. Res.* **2006**, *39*, 465-475.
- ³ Gales, P.A.; Quesada, R. *Coord. Chem. Rev.* **2006**, *250*, 3219-3244.
- ⁴ Snowden, T.S.; Anslyn, E.V. *Curr. Opin. Chem. Biol* **1999**, *3*, 740-746.
- ⁵ Lui, W-X.; Jiang, Y-B. *Org. Biomol. Chem.* **2007**, *5*, 1771-1775.
- ⁶ Quinlan, E.; Matthews, S.E.; Gunnlaugsson, T. *Tetrahedron Lett.* **2006**, 9333-9338.
- ⁷ Diaz, P.; Mingos, D.M.P.; Vilar, R.; White, A.J.P.; Williams, D.J. *Inorg. Chem.* **2004**, *43*, 7597-7604.
- ⁸ Park, C.H.; Simmons, H.E. *J. Am. Chem. Soc.* **1968**, *90*, 2431-2432.
- ⁹ Albrecht, M. *Naturwissenschaften* **2007**, *94*, 951-966.
- ¹⁰ Bowman-James, K. *Acc. Chem. Res.* **2005**, *38*, 671-678.
- ¹¹ Kang, S.O.; Begum, R.A.; Bowman-James, K. *Angew. Chem. Int. Ed.* **2006**, *45*, 7882-7894.
- ¹² Ilioudis, C.A.; Tocher, D.A.; Steed, J.W. *J. Am. Chem. Soc.* **2004**, *126*, 12395-12402.
- ¹³ Smith, P.J.; Reddington, M.V.; Wilcox, C.S. *Tetrahedron Lett.* **1992**, *33*, 6085-6088.
- ¹⁴ Fan, E.; Van Arman, S.A.; Kincaid, S.; Hamilton, A.D. *J. Am. Chem. Soc.* **1993**, *115*, 369-370.
- ¹⁵ Brooks, S.J.; Edwards, P.R.; Gale, P.A.; Light, M.E. *New J. Chem.* **2006**, *30*, 65-70
- ¹⁶ Amendola, V.; Bonizzoni, M.; Esteban-Gomez, D.; Fabbriizzi, L.; Licchelli, M.; Sancenon, F.; Taglietti, A. *Coord. Chem. Rev.* **2006**, *250*, 1451-1470.
- ¹⁷ Pratt, M.D.; Beer, P.D. *Polyhedron* **2003**, *22*, 649-653.
- ¹⁸ Huang, Y-L.; Hung, W-C.; Lai, C-C.; Liu, Y-H.; Peng, S-M.; Chiu, S-H. *Angew. Chem. Int. Ed.* **2007**, *46*, 6629-6633.
- ¹⁹ Kavallieratos, K.; Bertao, C.M.; Crabtree, R.H. *J. Org. Chem.* **1999**, *64*, 1675-1683.
- ²⁰ Kavallieratos, K.; de Gala, S.R.; Austin, D.J.; Crabtree, R.H. *J. Am. Chem. Soc.* **1997**, *119*, 2325-2326.
- ²¹ Coles, S.J.; Frey, J.G.; Gale, P.A.; Hursthouse, M.B.; Light, M.E.; Navakhun, K.; Thomas, G.L. *Chem. Commun.* **2003**, 568-569.

- ²² Hughes, M.P.; Smith, B.D. *J. Org. Chem.* **1997**, *62*, 4492-4499.
- ²³ Kondo, S.; Suzuki, T.; Yano, Y. *Tetrahedron Lett.* **2002**, *43*, 7059-7061.
- ²⁴ a) Deetz, M.J.; Shang, M.; Smith, B.D. *J. Am. Chem. Soc.* **2000**, *122*, 6201-6207. b) Mahoney, J.M.; Beatty, A.M.; Smith, D.B. *J. Am. Chem. Soc.* **2001**, *123*, 5847-5848.
- ²⁵ Mahoney, J.M.; Beatty, A.M.; Smith, B.D. *Inorg. Chem.* **2004**, *43*, 7617-7621.
- ²⁶ Mahoney, J.M.; Davis, J.P.; Beatty, A.M.; Smith, D.B. *J. Org. Chem.* **2003**, *68*, 9819-9820.
- ²⁷ a) Chang, S.; Hamilton, A.D. *J. Am. Chem. Soc.* **1988**, *110*, 1318-1319. b) Garcia-Tellado, F.; Goswami, S.; Chang, S.; Geib, S.J.; Hamilton, A.D. *J. Am. Chem. Soc.* **1990**, *112*, 7393-7394. c) Chang, S.; Engen, D.V.; Fan, E.; Hamilton, A.D. *J. Am. Chem. Soc.* **1991**, *113*, 7640-7645.
- ²⁸ Hunter, C.A.; Purvis, D.H. *Angew. Chem. Int. Ed. Engl.* **1992**, *31*, 792-795.
- ²⁹ Chmielewski, M.J.; Zielinski, T.; Jurczak, J. *Pure. Appl. Chem.* **2007**, *79*, 1087-1096.
- ³⁰ Keaveney, C.M.; Leigh, D.A. *Angew. Chem. Int. Ed.* **2004**, *43*, 1222.
- ³¹ Xiao, S.; Fu, N.; Peckham, K.; Smith, B.D. *Org. Lett.* **2010**, *12*, 140-143.
- ³² a) Hunter, C.A. *J. Am. Chem. Soc.* **1992**, *114*, 5303-5311. b) Vögtle, F.; Meier, S.; Hoss, R. *Angew. Chem. Int. Ed.* **1992**, *31*, 1619-1622. c) Johnston, A.G.; Leigh, D.A.; Nezhat, L.; Smart, J.P.; Deegan, M.D. *Angew. Chem. Int. Ed.* **1995**, *34*, 1212-1216.
- ³³ Kidd, T.J.; Leigh, D.A.; Wilson, A.J. *J. Am. Chem. Soc.* **1999**, *121*, 1599-1600.
- ³⁴ a) Wisner, J.A.; Beer, P.D.; Drew, M.G.B. *Angew. Chem. Int. Ed.* **2001**, *40*, 3606-3609. b) Wisner, J.A.; Beer, P.D.; Berry, N.G.; Tomapatanaget, B. *Proc. Natl. Acad. Sci.* **2002**, *99*, 4983-4986.
- ³⁵ Wisner, J.A.; Beer, P.D.; Drew, M.G.B.; Sambrook, M.R. *J. Am. Chem. Soc.* **2002**, *124*, 12469-12476.
- ³⁶ Sambrook, M.R.; Beer, P.D.; Wisner, J.A.; Paul, R.L.; Cowley, A.R. *J. Am. Chem. Soc.* **2004**, *126*, 15364-15365.
- ³⁷ Ramos, S.; Alcalde, E.; Doddi, G.; Mencarelli, P.; Perez-Garcia, L.; *J. Org. Chem.* **2002**, *67*, 8463-8468.
- ³⁸ a) Hasenknopf, B.; Lehn, J.-M.; Boumediene, N.; Dupont-Gervais, A.; Van Dorsselaer, A.; Kneisel, B.; Fenske, D. *J. Am. Chem. Soc.* **1997**, *119*, 10956-10962. b)

- Hasenknopf, B.; Lehn, J-M.; Boumediene, N.; Leize, E.; Van Dorsselaer, A. *Angew. Chem. Int. Ed.* **1998**, *37*, 3265-3268.
- ³⁹ Vilar, R.; Mingos, D.M.P.; White, A.J.P.; Williams, D.J. *Angew. Chem. Int. Ed.* **1998**, *37*, 1258-1261.
- ⁴⁰ Diaz, P.; Mingos, D.M.P.; Vilar, R.; White, A.J.P.; Williams, D.J. *Inorg. Chem.* **2004**, *43*, 7597-7604.
- ⁴¹ a) Curiel, D.; Beer, P.D.; Paul, R.L.; Cowley, A.; Sambrook, M.R.; Szemes, F. *Chem. Commun.* **2004**, 1162-1163. b) Curiel, D.; Beer, P.D. *Chem. Commun.* **2005**, 1909-1911.
- ⁴² Hübner, G.M.; Gläser, J.; Seel, C.; Vögtle, F. *Angew. Chem. Int. Ed.* **1999**, *38*, 383-386.
- ⁴³ Haussmann, P.C.; Khan, S.I.; Stoddart, J.F. *J. Org. Chem.* **2007**, *72*, 6708-6713.
- ⁴⁴ Glink, P.T.; Oliva, A.I.; Stoddart, J.F.; White, A.J.P.; Williams, D.J. *Angew. Chem. Int. Ed.* **2001**, *40*, 1870-1875.
- ⁴⁵ Corbett, P.T.; Leclaire, J.; Vial, L.; West, K.R.; Wietor, J-L.; Sanders, J.K.M.; Otto, S. *Chem. Rev.* **2006**, *106*, 3652-3711.
- ⁴⁶ Rowan, S.J.; Cantrill, S.J.; Cousins, G.R.L.; Sanders, J.K.M.; Stoddart, J.F. *Angew. Chem. Int. Ed.* **2002**, *41*, 898-952.
- ⁴⁷ Rowan, S.J.; Lukeman, P.S.; Reynolds, D.J.; Sanders, J.K.M. *New. J. Chem.* **1998**, *22*, 1015-1018.
- ⁴⁸ Larsson, R.; Ramström, O. *Eur. J. Org. Chem.* **2006**, 285-291.
- ⁴⁹ Drahoňovský, D.; Lehn, J-M. *J. Org. Chem.* **2009**, *74*, 8428-8432.
- ⁵⁰ a) Otto, S.; Kubik, S. *J. Am. Chem. Soc.* **2003**, *125*, 7804-7805. b) Corbett, P.T.; Sanders, J.K.M.; Otto, S. *J. Am. Chem. Soc.* **2005**, *127*, 9390-9392. c) Otto, S.; Furlan, R.L.E.; Sanders, J.K.M. *J. Am. Chem. Soc.* **2000**, *122*, 12063-12064.
- ⁵¹ Nazarpack-Kandlousy, N.; Zweigenbaum, J.; Henion, J.; Eliseev, A.V. *J. Comb. Chem.* **1999**, *1*, 199-206.
- ⁵² Huc, I.; Lehn, J-M. *Proc. Natl. Acad. Sci.* **1997**, *94*, 2106-2110.
- ⁵³ Cantrill, S.J.; Rowan, S.J.; Stoddart, J.F. *Org. Lett.* **1999**, *1*, 1363-1366.

- ⁵⁴ Klivansky, L.M.; Koshkakarayan, G.; Cao, D.; Liu, Y. *Angew. Chem. Int. Ed.* **2009**, *48*, 4185-4189.
- ⁵⁵ Ro, S.; Rowan, S.J.; Pease, A.R.; Cram, D.J.; Stoddart, J.F. *Org. Lett.* **2000**, *2*, 2411-2414.
- ⁵⁶ Quan, M.L.C.; Cram, D.J. *J. Am. Chem. Soc.* **1991**, *113*, 2754-2755.
- ⁵⁷ Jurczak, J.; Ziach, K. *Org. Lett.* **2008**, *10*, 5159-5162.
- ⁵⁸ a) Thompson, M.C.; Busch, D.H. *J. Am. Chem. Soc.* **1962**, *84*, 1762-1763. b) Sessler, J.L.; Mody, T.D.; Lynch, V. *Inorg. Chem.* **1992**, *31*, 529-531. c) Wang, Z.; Reibenspies, J.; Martell, A.E. *Inorg. Chem.* **1997**, *36*, 629-636. d) Epstein, D.M.; Choudhary, S.; Churchill, M.R.; Keil, K.M.; Eliseev, A.V.; Morrow, J.R. *Inorg. Chem.* **2001**, *40*, 1591-1596. e) Leung, A.C.W.; MacLachlan, M.J. *J. Inorg. Organomet. Polym., Mater.* **2007**, *17*, 57-89.
- ⁵⁹ Wessjohann, L.A.; Rivera, D.G.; León, F. *Org. Lett.* **2007**, *9*, 4733-4736.
- ⁶⁰ Cousins, G.R.L.; Poulsen, S-A.; Sanders, J.K.M. *Chem. Commun.* **1999**, 1575-1576.
- ⁶¹ Furlan, R.L.E.; Ng, Y-F.; Otto, S.; Sanders, J.K.M. *J. Am. Chem. Soc.* **2001**, *123*, 8876-8877.
- ⁶² Roberts, S.L.; Furlan, R.L.E.; Otto, S.; Sanders, J.K.M. *Org. Biomol. Chem.* **2003**, *1*, 1625-1633.
- ⁶³ a) Cousins, G.R.L.; Furlan, R.L.E.; Ng, Y-F.; Redman, J.E.; Sanders, J.K.M. *Angew. Chem. Int. Ed.* **2001**, *40*, 423-428. b) Furlan, R.L.E., Ng., Y-F.; Cousins, G.R.L.; Redman, J.E.; Sanders, J.K.M. *Tetrahedron* **2002**, *58*, 771-778.
- ⁶⁴ Lam, R.T.S.; Belenguer, A.; Roberts, S.L.; Naumann, C.; Jarrosson, T.; Otto, S.; Sanders, J.K.M. *Science* **2005**, *308*, 667-669.
- ⁶⁵ Chung, M-K.; White, P.S.; Lee, S.J.; Gagné, M.R. *Angew. Chem. Int. Ed.* **2009**, *48*, 8683-8686.
- ⁶⁶ Simpson, M.G.; Watson, S.P.; Feeder, N.; Davies, J.E.; Sanders, J.K.M. *Org. Lett.* **2000**, *2*, 1435-1438.
- ⁶⁷ Berl, V.; Huc, I.; Lehn, J-M.; DeCaian, A.; Fischer, J. *Eur. J. Org. Chem.* **1999**, 3089-3094.

- ⁶⁸ a) Katayev, E.A.; Pantos, G.D.; Reshetova, M.D.; Khrustalev, V.N.; Lynch, V.M.; Ustynyuk, Y.A.; Sessler, J.L. *Angew. Chem. Int. Ed.* **2005**, *44*, 7386-7390. b) Katayev, E.A.; Boev, N.V.; Myshkovskaya, E.; Khrustalev, V.N.; Ustynyuk, Y.A. *Chem. Eur. J.* **2008**, *14*, 9065-9073.
- ⁶⁹ Schiff, H. *Just. Liebigs. Ann. Chem.* **1864**, *131*, 118-119.
- ⁷⁰ Layer, R.W. *Chem. Rev.* **1963**, *63*, 489-510.
- ⁷¹ Swain, C.G.; Worosz, J.C. *Tett. Lett.* **1965**, *6*, 3199-3202.
- ⁷² Cordes, E.H.; Jencks, W.P. *J. Am. Chem. Soc.* **1962**, *84*, 832-837.
- ⁷³ Chaturvedi, R.K.; Cordes, E.H. *J. Am. Chem. Soc.* **1967**, *89*, 4631-4637.
- ⁷⁴ Young, P.R.; Howell, L.G.; Owen, T.C. *J. Am. Chem. Soc.* **1975**, *97*, 6544-6551.
- ⁷⁵ Pino, T.; Cordes, E.H. *J. Org. Chem.* **1971**, *36*, 1668-1670.
- ⁷⁶ a) Bru, M.; Alfonso, I.; Burguete, M. I.; Luis, S.V. *Angew. Chem. Int. Ed.* **2006**, *45*, 6155-6159. b) Alfonso, I.; Bolte, M.; Bru, M.; Burguete, M.I.; Luis, S.V.; Rubio, J. *J. Am. Chem. Soc.* **2008**, *130*, 6137-6144.
- ⁷⁷ Giuseppone, N.; Schmitt, J-L.; Shwartz, E.; Lehn, J-M. *J. Am. Chem. Soc.* **2005**, *127*, 5528-5539.
- ⁷⁸ Gupta, V.K.; Goyal, R.N.; Sharma, R.A. *Talanta* **2008**, *76*, 859-864.
- ⁷⁹ Wang, Y-H.; Hai, L.; Lin, H-K. *Chinese Journal of Chemistry* **2007**, *25*, 1430-1433.
- ⁸⁰ Chawla, H.M.; Sahu, S.N.; Shrivastava, R. *Tetrahedron Lett.* **2007**, *48*, 6054-6058.
- ⁸¹ Chawla, H.M.; Singh, S.P.; *Tetrahedron* **2008**, *64*, 741-748.
- ⁸² Minkkila, A.; Myllymaki, M.J.; Saario, S.M.; Castillo-Melendez, J.A.; Koskinen, A.M.P.; Fowler, C.J.; Leppanen, J.; Nevalainen, T. *Eur. J. Med. Chem.* **2009**, *44*, 2994-3008.
- ⁸³ Hoshino, O.; Saito, K.; Ishizaki, M.; Umezawa, B. *Synth. Commun.* **1987**, *17*, 1887-1892.
- ⁸⁴ Sander, E.G.; Jencks, W.P. *J. Am. Chem. Soc.* **1968**, *90*, 6154-6162.
- ⁸⁵ Smith, M.B.; March, J. *March's Advanced Organic Chemistry, 6th ed.*; John Wiley & Sons Inc.: New Jersey, USA, 2007.